doi:10.1007/s10495-009-0341-y

[4] S. Oyadomari and M. Mori, "Roles of CHOP/GADD153 in Endoplasmic Reticulum Stress," *Cell Death and Differentiation,* Vol. 11, No. 4, 2004, pp. 381-389. doi:10.1038/sj.cdd.4401373

[5] R. S. Saliba, P. M. Munro, P. J. Luthert and M. E. Chee-tham, "The Cellular Fate of Mutant Rhodopsin: Quality Control, Degradation and Aggresome Formation," *Journal of cell science*, Vol. 115, No. Pt 14, 2002, pp. 2907-2918.

[6] E. H. Koo, P. T. Lansbury, Jr. and J. W. Kelly, "Amyloid Diseases: Abnormal Protein Aggregation in Neurodegenera-tion," *Proceedings of the National Academy of Sciences of the United States of America*, Vol. 96, No. 18, 1999, pp. 9989-9990. doi:10.1073/pnas.96.18.9989

[7] C. Kakiuchi, K. Iwamoto, M. Ishiwata, M. Bundo, T. Kasahara, I. Kusumi, T. Tsujita, Y. Okazaki, S. Nanko, H. Kunugi, T. Sasaki and T. Kato, "Impaired Feedback Regulation of XBP1 as a Genetic Risk Factor for Bipolar disorder,"*Nature Genetics*, Vol. 35, No. 2, 2003, pp. 171-175. doi:10.1038/ng1235

[8] C. Kakiuchi, M. Ishiwata, T. Umekage, M. Tochigi, K. Kohda, T. Sasaki and T. Kato, "Association of the XBP1-116C/G Polymorphism with Schizophrenia in the Japanese Population," *Psychiatry and Clinical Neurosciences*, Vol. 58, No. 4, 2004, pp. 438-440. doi:10.1111/j.1440-1819.2004.01280.x

[9] L. Shao, X. Sun, L. Xu, L. T. Young and J. F. Wang, "Mood Stabilizing Drug Lithium Increases Expression of Endoplasmic Reticulum Stress Proteins in Primary Cultured Rat Cerebral Cortical Cells," *Life Sciences*, Vol. 78, No. 12, 2006, pp. 1317-1323. doi:10.1016/j.lfs.2005.07.007

[10] S. Kurosawa, E. Hashimoto, W. Ukai, S. Toki, S. Saito and T. Saito, "Olanzapine Potentiates Neuronal Survival and Neural Stem Cell Differentiation: Regulation of Endo-plasmic Reticulum Stress Response Proteins," *Journal of Neural Transmission*, Vol. 114, No. 9, 2007, pp. 1121- 1128. doi:10.1007/s00702-007-0747-z

[11] C. Bown, J. F. Wang, G. MacQueen and L. T. Young, "Increased Temporal Cortex ER Stress Proteins in Depressed Subjects Who Died by Suicide," Neuropsychopharmacology, Vol. 22, No. 3, 2000, pp. 327-332. doi:10.1016/S0893-133X(99)00091-3

[12] Y. I. Sheline, P. W. Wang, M. H. Gado, J. G. Csernansky and M. W. Vannier, "Hippocampal Atrophy in Recurrent Major Depression," *Proceedings of the National Academy of Sciences of the United States of America*, Vol. 93, No. 9, 1996, pp. 3908-3913. doi:10.1073/pnas.93.9.3908

[13] D. Ongur, W. C. Drevets and J. L. Price, "Glial Reduction in the Subgenual Prefrontal Cortex in Mood Disorders," *Proceedings of the National Academy of Sciences of the United States of America*, Vol. 95, No. 22, 1998, pp. 13290-13295. doi:10.1073/pnas.95.22.13290

[14] Y. Watanabe, E. Gould and B. S. McEwen, "Stress Induces Atrophy of Apical Dendrites of Hippocampal CA3 Pyramidal Neurons," *Brain research*, Vol. 588, No. 2, 1992, pp. 341-345. doi:10.1016/0006-8993(92)91597-8

[15] A. Bachis, M. I. Cruz, R. L. Nosheny and I. Mocchetti, "Chronic Unpredictable Stress Promotes Neuronal Apoptosis in the Cerebral Cortex," *Neuroscience Letters*, Vol. 442, No. 2, 2008, pp. 104-108. doi:10.1016/j.neulet.2008.06.081

[16] D. Chen, E. Padiernos, F. Ding, I. S. Lossos and C. D. Lopez, "Apoptosis-stimulating Protein of P53-2 (ASPP2/53BP2L) is an E2F Target Gene," *Cell Death and Differentiation*, Vol. 12, No. 4, 2005, pp. 358-368. doi:10.1038/sj.cdd.4401536

[17] O. I. Abatan, K. B. Welch and J. A. Nemzek, "Evaluation of Saphenous Venipuncture and Modified Tail-clip Blood Collection in Mice," *Journal of the American Association for Laboratory Animal Science,*, Vol. 47, No. 3, 2008, pp. 8-15.

[18] S. L. Gourley and J. R. Taylor, "Recapitulation and Reversal of a Persistent Depression-like Syndrome in Rodents," *Current Protocols in Neuroscience* Chapter 9, 2009, Unit-9.32.

[19] X. Z. Wang, B. Lawson, J. W. Brewer, H. Zinszner, A. Sanjay, L. J. Mi, R. Boorstein, G. Kreibich, L. M. Hendershot and D. Ron, "Signals from the Stressed Endoplasmic Reticulum Induce C/EBP-homologous Protein (CHOP/GADD153)," *Molecular and Cellular Biology*, Vol. 16, No. 8, 1996, pp. 4273-4280.

[20] H. Zinszner, M. Kuroda, X. Wang, N. Batchvarova, R. T. Lightfoot, H. Remotti, J. L. Stevens and D. Ron, "CHOP is Implicated in Programmed Cell Death in Response to Impaired Function of the Endoplasmic Reticulum," *Genes & Development*, Vol. 12, No. 7, 1998, pp. 982-995. doi:10.1101/gad.12.7.982

[21] M. Cechowska-Pasko, "Endoplasmic Reticulum Chaperons," *Postepy Biochemii*, Vol. 55, No. 4, 2009, pp. 416-424.

[22] C. A. Sandman, J. L. Barron and L. Parker, "Disregulation of Hypothalamic-pituitary-adrenal Axis in the Mentally Retarded," *Pharmacology, Biochemistry, and Behavior*, Vol. 23, No. 1, 1985, pp. 21-26. doi:10.1016/0091-3057(85)90124-8

[23] A. Roy, "Hypothalamic-pituitary-adrenal Axis Function and Suicidal Behavior in Depression," Biological psychiatry, Vol. 32, No. 9, 1992, pp. 812-816. doi:10.1016/0006-3223(92)90084-D

[24] J. F. Lopez, D. M. Vazquez, D. T. Chalmers and S. J. Watson, "Regulation of 5-HT Receptors and the Hypothalamic-pituitary-adrenal Axis. Implications for the Neurobiology of Suicide," *Annals of the New York Academy of Sciences*, Vol. 836, No. 1, 1997, pp. 106-134.

[25] J. Y. Zhou, H. J. Zhong, C. Yang, J. Yan, H. Y. Wang and J. X. Jiang, "Corticosterone Exerts Immunostimulatory Effects on Macrophages via Endoplasmic Reticulum Stress," *The British Journal of Surgery*, Vol. 97, No. 2, 2010, pp. 281-293. doi:10.1002/bjs.6820

[26] J. Du, B. McEwen and H. K. Manji, "Glucocorticoid Receptors Modulate Mitochondrial Function: A Novel Mechanism for Neuroprotection," *Communicative & In-*

tegrative Biology, Vol. 2, No. 4, 2009, pp. 350-352.

[27] J. Du, Y. Wang, R. Hunter, Y. Wei, R. Blumenthal, C. Falke, R. Khairova, R. Zhou, P. Yuan, R. Machado-Vieira, B. S. McEwen and H. K. Manji, "Dynamic Regulation of Mitochondrial Function by Glucocorticoids," *Proceedings of the National Academy of Sciences of the United States of America*, Vol. 106, No. 9, 2009, pp. 3543-3548. doi:10.1073/pnas.0812671106

[28] H. Coe and M. Michalak, "Calcium Binding Chaperones of the Endoplasmic Reticulum," *General Physiology and Biophysics*, Vol. 28 Spec No Focus, 2009, pp. 96- 103.

[29] N. Galeotti, A. Bartolini and C. Ghelardini, "Blockade of Intracellular Calcium Release Induces an Antidepressant-like Effect in the Mouse Forced Swimming Test," *Neuropharmacology*, Vol. 50, No. 3, 2006, pp. 309-316. doi:10.1016/j.neuropharm.2005.09.005

[30] S. L. Gourley, F. J. Wu, D. D. Kiraly, J. E. Ploski, A. T. Kedves, R. S. Duman and J. R. Taylor, "Regionally Specific Regulation of ERK MAP Kinase in a Model of Antidepressant-sensitive Chronic Depression," Biological psychiatry, Vol. 63, No. 4, 2008, pp. 353-359. doi:10.1016/j.biopsych.2007.07.016

[31] T. Ito, N. Morita, M. Nishi and M. Kawata, "In Vitro and in Vivo Immunocytochemistry for the Distribution of Mineralocorticoid Receptor with the Use of Specific Antibody," *Neuroscience Research*, Vol. 37, No. 3, 2000, pp. 173-182. doi:10.1016/S0168-0102(00)00112-7

[32] F. Han, H. Ozawa, K. Matsuda, M. Nishi and M. Kawata, "Colocalization of Mineralocorticoid Receptor and Glucocorticoid Receptor in the Hippocampus and Hypothalamus," *Neuroscience Research*, Vol. 51, No. 4, 2005, pp. 371-381. doi:10.1016/j.neures.2004.12.013

[33] P. J. Lucassen, W. Scheper and E. J. Van Someren, "Adult Neurogenesis and the Unfolded Protein Response; New Cellular and Molecular Avenues in Sleep Research," *Sleep Medicine Reviews*, Vol. 13, No. 3, 2009, pp. 183-186. doi:10.1016/j.smrv.2008.12.004

[34] G. Chen, Z. Fan, X. Wang, C. Ma, K. A. Bower, X. Shi, Z. J. Ke and J. Luo, "Brain-derived Neurotrophic Factor Suppresses Tunicamycin-induced Upregulation of CHOP in Neurons," *Journal of Neuroscience Research*, Vol. 85, No. 8, 2007, pp. 1674-1684. doi:10.1002/jnr.21292

Mamm Genome (2011) 22:318–328
DOI 10.1007/s00335-011-9329-3

ENU-induced missense mutation in the C-propeptide coding region of *Col2a1* creates a mouse model of platyspondylic lethal skeletal dysplasia, Torrance type

Tatsuya Furuichi · Hiroshi Masuya · Tomohiko Murakami · Keiichiro Nishida · Gen Nishimura · Tomohiro Suzuki · Kazunori Imaizumi · Takashi Kudo · Kiyoshi Ohkawa · Shigeharu Wakana · Shiro Ikegawa

Received: 12 February 2011 / Accepted: 14 April 2011 / Published online: 3 May 2011

Abstract The *COL2A1* gene encodes the α1(II) chain of the homotrimeric type II collagen, the most abundant protein in cartilage. In humans, *COL2A1* mutations create many clinical phenotypes collectively termed type II collagenopathies; however, the genetic basis of the phenotypic diversity is not well elucidated. Therefore, animal models corresponding to multiple type II collagenopathies are required. In this study we identified a novel *Col2a1* missense mutation—c.44406A>C (p.D1469A)—produced by large-scale *N*-ethyl-*N*-nitrosourea (ENU) mutagenesis in a mouse line. This mutation was located in the C-propeptide coding region of *Col2a1* and in the positions corresponding to a human *COL2A1* mutation responsible for platyspondylic lethal skeletal dysplasia, Torrance type (PLSD-T). The phenotype was inherited as a semidominant trait. The heterozygotes were mildly but significantly smaller than wild-type mice. The homozygotes exhibited lethal skeletal dysplasias, including extremely short limbs, severe spondylar dysplasia, severe pelvic hypoplasia, and brachydactyly. As expected, these skeletal defects in the homozygotes were similar to those in PLSD-T patients. The secretion of the mutant proteins into the extracellular space was disrupted, accompanied by abnormally expanded rough endoplasmic

Electronic Supplementary Material The online version of this article (doi:10.1007/s00335-011-9329-3) contains supplementary material, which is available to authorized users.

T. Furuichi (✉) · K. Ohkawa
Laboratory Animal Facility, Research Center for Medical Sciences, Jikei University School of Medicine, 3-25-8 Nishi-shinbashi, Minato-ku, Tokyo 105-8461, Japan
e-mail: furuichi@jikei.ac.jp

T. Furuichi · S. Ikegawa
Laboratory for Bone and Joint Diseases, Center for Genomic Medicine, RIKEN, 4-6-1 Shirokanedai, Minato-ku, Tokyo 108-8639, Japan

H. Masuya
Technology and Development Unit for Knowledge Base of Mouse Phenotype, RIKEN Bioresource Center, 3-1-1 Koyadai, Tsukuba, Ibaraki 305-0074, Japan

T. Murakami
Division of Molecular and Cellular Biology, Department of Anatomy, Faculty of Medicine, University of Miyazaki, 5200 Kihara, Kiyotake, Miyazaki 889-1692, Japan

K. Nishida
Department of Human Morphology, Okayama University Graduate School of Medicine, Dentistry and Pharmaceutical Sciences, 2-5-1 Shikata-cho, Okayama 700-8558, Japan

G. Nishimura
Department of Pediatric Imaging, Tokyo Metropolitan Children's Medical Center, 2-8-9 Musashidai, Futyu, Tokyo 183-8561, Japan

T. Suzuki · S. Wakana
Technology and Development Team for Mouse Phenotype Analysis, Japan Mouse Clinic, RIKEN Bioresource Center, 3-1-1 Koyadai, Tsukuba, Ibaraki 305-0074, Japan

K. Imaizumi
Department of Biochemistry, Graduate School of Biomedical Science, Hiroshima University, 1-2-3 Kasumi, Minami-ku, Hiroshima 734-8553, Japan

T. Kudo
Department of Psychiatry and Behavioral Science, Osaka University Graduate School of Medicine, 2-2 Yamadaoka, Suita, Osaka 565-0871, Japan

reticulum (ER) and upregulation of ER stress-related genes, such as *Grp94* and *Chop*, in chondrocytes. These findings suggested that the accumulation of mutant type II collagen in the ER and subsequent induction of ER stress are involved, at least in part in the PLSD-T–like phenotypes of the mutants. This mutant should serve as a good model for studying PLSD-T pathogenesis and the mechanisms that create the great diversity of type II collagenopathies.

Introduction

Type II collagen is the most abundant protein in cartilage and, along with other tissue-specific collagens and proteoglycans, provides structural integrity to tissue (Myllyharju and Kivirikko 2004; Olsen 1995). This fibrillar collagen is a homotrimer composed of three collagen α1(II) chains containing segments with a characteristic Gly-X-Y repeat sequence that forms a triple-helical structure. As with other fibrillar collagen chains, these chains are synthesized as procollagen, which contains noncollagenous domains at both the N- and C-termini. The C-terminal noncollagenous domain, termed C-propeptide, is essential for triple-helical formation (Doege and Fessler 1986; Khoshnoodi et al. 2006). After being secreted into the extracellular space, the noncollagenous domains of both ends are cleaved by specific proteinases.

COL2A1 encodes the collagen α1(II) chain, and in humans, heterozygous mutations in this gene lead to many clinical phenotypes collectively termed type II collagenopathies (Kuivaniemi et al. 1997; Nishimura et al. 2005). Most *COL2A1* mutations have been identified in the coding region of the triple-helical domain. Truncation mutations in this region produce Sticker dysplasia type-I (STD-I) or Kniest dysplasia (KND) (Ahmad et al. 1991; Winterpacht et al. 1993), and missense mutations cause a spectrum of spondyloepiphyseal dysplasia (SED) or hypochondrogenesis (HCG) (Korkko et al. 2000; Nishimura et al. 2005). Mutations in the C-propeptide coding region are not common and produce variable clinical phenotypes such as platyspondylic lethal skeletal dysplasia, Torrance type (PLSD-T) (Nishimura et al. 2004; Zankl et al. 2005), spondyloperipheral dysplasia (SPPD) (Zabel et al. 1996), SED congenital (SEDC) (Unger et al. 2001), and HCG (Mortier et al. 2000).

The disproportionate micromelia (*Dmm*) mouse, generated by radiation-induced mutagenesis, is the only known example of an animal model possessing endogenous mutations in the C-propeptide coding region of *Col2a1* (Brown et al. 1981; Pace et al. 1997). A 3-bp deletion, substituting Lys and Thr with Asn (p.K1448_T1449delinsN), was identified in this mutant (Pace et al. 1997). The homozygotes have severe skeletal dysplasia and die at birth because of thoracic insufficiency. The heterozygotes appear normal at birth, exhibit only a mild dwarfism beginning at 1 week of age, and develop early-onset osteoarthritis (OA) that becomes conspicuous at 3 months of age (Bomsta et al. 2006). To understand at the molecular level the phenotypic diversity of type II collagenopathies with C-propeptide mutations, additional animal models corresponding to PLSD-T, SPPD, SEDC, and HGG phenotypes are required.

In this study we identified a novel *Col2a1* mouse mutant carrying a missense mutation in the C-propeptide coding region that was produced by a large-scale *N*-ethyl-*N*-nitrosourea (ENU) mutagenesis program (Inoue et al. 2004; Masuya et al. 2005a, b, 2007). The amino acid residue resulting from this mutation corresponded to that of human *COL2A1* mutations responsible for PLSD-T. As expected, the skeletal defects of the homozygous mice were similar to those of PLSD-T patients. This mouse will be a good tool for studying PLSD-T pathogenesis and the mechanisms that create the great diversity of type II collagenopathies.

Materials and methods

ENU mutagenesis, inheritance testing, and gene mapping

The method for mouse ENU mutagenesis is available at http://www.brc.riken.go.jp/lab/gsc/mouse/ and in previous reports (Inoue et al. 2004; Masuya et al. 2005a, b, 2007). C57BL/6J and DBA/2J mice were purchased from CLEA Japan (Tokyo, Japan). C57BL/6J males administered ENU (total dosage of 150–250 mg/kg) were crossed to DBA/2J females. The resultant F1 hybrids (G1 animals) were subjected to screening for various phenotypes at 8 weeks of age. Examination of adult limb phenotype was performed as a subtest of the modified-SHIRPA protocol, a comprehensive package of screens for morphological and behavioral phenotypes (Masuya et al. 2005a). A complete list of the subtests is available at the above website. M100856 mouse lines were crossed with wild-type DBA/2J mice to test for phenotype transmission and for genetic mapping of the causative genes. Genomic DNA was prepared from the tail tips of the G2 progeny using the NA-2000 automatic nucleic acid isolation system (KURABO, Osaka, Japan). We used the db-SNP website (http://www.ncbi.nlm.nih.gov/entrez/query.fcgi?db=snp) for single nucleotide polymorphisms (SNPs) and the microsatellite markers listed on the MGI website (http://www.informatics.jax.org/) for simple sequence length polymorphisms. Polymorphic loci were examined using TaqMan MGB assays on the ABI

7700 and ABI 7900 Sequence Detection Systems (Applied Biosystems, Foster City, CA, USA).

Mutation screening and genotyping

We searched for *Col2a1* mutations using cDNAs derived from M100856 lines. We amplified by PCR seven overlapping cDNA fragments that cover the entire coding region and sequenced the PCR products with an ABI 3700 automated sequencer (Applied Biosystems). PCR conditions and primer sequences are available upon request. For the mutation numbering, +1 corresponds to the A of the ATG translation initiation codon in mouse *Col2a1* NCBI reference sequence NM_031163.3. Genotyping of the identified mutant allele *Col2a1*^{Rgsc856} was performed by sequencing the PCR products amplified with the following primer pair: 5′-AAGTTCTAGCAAGCCACCCA-3′ and 5′-AGGACGGTTGGGTATCATCA-3′.

Skeletal analysis

Embryos were eviscerated and fixed in 99% EtOH for 4 days. Alcian blue staining was performed in a solution of 80% EtOH, 20% acetic acid, and 0.015% Alcian blue for 4 days at 37°C. Specimens were rinsed and soaked in 95% EtOH for 3 days. Alizarin red staining was then performed in a solution of 0.002% alizarin red and 1% KOH for 12 h at room temperature. After rinsing with water, specimens were kept in 1% KOH solution until the skeletons became clearly visible. For storage, specimens were transferred into 50, 80, and finally 100% glycerol.

Histological and immunohistochemical analysis

For histological analysis of mouse embryos, limbs were fixed in 4% paraformaldehyde (PFA) and decalcified in 10% EDTA for a week at 4°C. Hematoxylin & eosin (HE) and toluidine blue staining were performed using 6-μm paraffin sections according to standard protocols. For immunohistochemistry, paraffin sections were incubated with rabbit anti-type II collagen (Acris Antibodies, Hiddenhausen, Germany) or mouse anti-KDEL (MBL, Nagoya, Japan) antibodies. Primary antibodies were visualized with Alexa-conjugated goat anti-rabbit IgG (Molecular Probes®, Invitrogen, Carlsbad, CA, USA) and fluorescein-conjugated goat anti-mouse IgG antibodies (ICN Pharmaceuticals, Aliso Viejo, CA, USA). Stained cells were viewed using a fluorescence microscope or a confocal microscope (FV1000D; Olympus, Tokyo, Japan). To examine whether *Col2a1*^{Rgsc856} heterozygotes develop early-onset OA, knee and elbow joint samples from mice at 10 months of age were dissected, fixed in 4% PFA for 24 h, and defatted in alcohol. Then the samples were decalcified in 0.3 M EDTA (pH 7.5) for 10 days. Safranin O staining was performed using 4.5-μm paraffin sections. The severity of the OA lesion was evaluated using the modified Mankin scoring system, as described previously (Mankin et al. 1971; van der Sluijs et al. 1992).

Electron microscope analysis

Limbs were fixed in 0.1 M sodium cacodylate buffer with 2.5% glutaraldehyde, decalcified in a 10% EDTA–Na_2 solution, and postfixed in 2% osmium tetroxide. After dehydration, they were embedded in EPON812. Semithin sections were stained with 1% toluidine blue to allow the selection of suitable areas for transmission electron microscopy. Ultrathin sections were stained with uranyl acetate and lead citrate. Visualization was performed using a Hitachi 7100 electron microscope (Hitachi, Tokyo, Japan) operated at 80 kV.

RT-PCR analysis

Total RNA was extracted from rib cartilages at embryonic day (E) 18.5 using ISOGEN (Nippongene, Tokyo, Japan). Equal amounts of total RNA were reverse-transcribed into cDNA using TaqMan Multiscribe Reverse Transcriptase (Applied Biosystems). Each reverse transcription reaction (1 μl) was used as a template for SYBR® Green real-time PCR (Qiagen, Valencia, CA, USA). The following primers were used for amplification: 5′-TGAAGCTGCAGTA GAGGAGG-3′ and 5′-GGATATAAGCCATGGGGTC A-3′ for *Grp94*; 5′-GAGTCCCTGCCTTTCACCTT-3′ and 5′-CTGTCAGCCAAGCTAGGGAC-3′ for *Chop*; and 5′-A ACTGGGACGACATGGAGAA-3′ and 5′-GGGGTGTTG AAGGTCTAAA-3′ for *Actb*. SYBR Green PCR and real-time fluorescence detection were performed using an ABI PRISM 7700 Sequence Detection System (Applied Biosystems).

Results

Identification of a novel *Col2a1* mutation located in the C-propeptide coding region

ENU is a highly potent chemical mutagen that randomly induces multiple single-base-pair changes in genomic DNA at a very high efficiency (approximately 1×10^{-3} per locus per gamete) (Hitotsumachi et al. 1985; Nolan et al. 1997). We screened 10,236 G1 mice (generated from crosses of ENU-mutagenized males and wild-type female mice) for abnormal skeletal phenotypes, especially focusing on the limb length transmitted as a dominant trait. We found one mutant line, termed M100856, that exhibits a

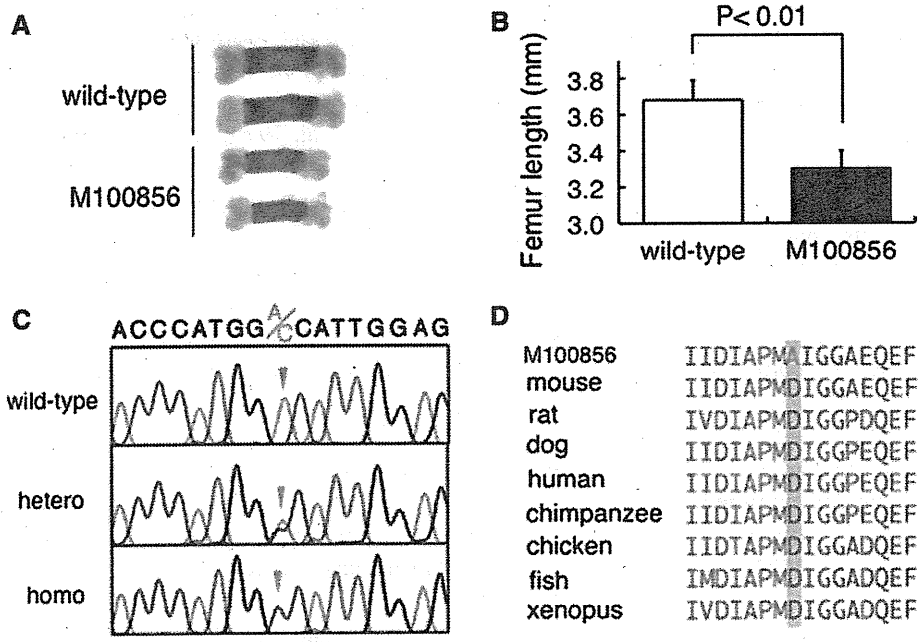

Fig. 1 Identification of a novel missense mutation in *Col2a1* in mice mutagenized with ENU. **a** Gross appearance of femurs from wild-type and M100856 mice at E18.5. **b** Length of femurs from wild-type and M100856 mice at E18.5. Data are expressed as the mean ± SD ($n = 5$). The p value was determined using Student's t-test. The same result was obtained from the independent experiment conducted using E19.5 embryos. **c** cDNA sequence chromatograms from wild-type mice, *M100856* heterozygotes, and *M100856* homozygotes. The location of the mutation is indicated by the *orange arrowhead*. **d** Comparison of the amino acid sequences around the D1469 residue in various species. Amino acid residues identical to mouse type II collagen are represented by *blue* letters and those not identical by *red* letters. The location of D1469 is indicated by *orange* shading. D1469 is highly conserved

short-limb phenotype (posted at http://www.brc.riken.go.jp/lab/gsc/mouse/) (Fig. 1a, b).

Linkage analysis using the 103 backcross progeny showed that the *M100856* locus was localized to a 2.9-cM region on chromosome 15 (Electronic Supplementary Fig. 1). We checked the functions of all genes located in the linkage region and found two genes that have important functions in skeletogenesis, i.e., *Col2a1* and *Vdr*. Because previously reported heterozygous *Col2a1* mutant mice exhibited very mild skeletal phenotypes similar to M100856 mouse (Brown et al. 1981; Donahue et al. 2003; Li et al. 1995), we chose *Col2a1* as the most likely candidate gene. Sequencing of *Col2a1* cDNA derived from M100856 mutant mouse identified a missense mutation—c.4406A>C—which is predicted to cause an Asp-to-Ala substitution at position 1469 (p.D1469A) (Fig. 1c). The mutation was located in the coding region of the C-propeptide. This Asp residue was strongly conserved throughout various species (Fig. 1d). Interestingly, the Asp residue corresponding to mouse D1469 was substituted in the human *COL2A1* mutation responsible for PLSD-T, i.e., p.D1469H (Zankl et al. 2005). The mutation was also confirmed by sequencing of genomic DNA and was not found in ten inbred mouse strains. No other alterations in the *Col2a1* coding region were found. We designated this novel *Col2a1* mutant allele found in the M100856 line as *Col2a1*^{Rgsc856}. The sequence chromatograms of the cDNA from *Col2a1*^{Rgsc856} heterozygotes showed no difference in expression levels between wild-type and mutant alleles (Fig. 1c). We sequenced all the coding exons and the flanking regions of the other candidate gene, *Vdr*, which encodes vitamin D receptor, in M100856 mutants but we did not find any mutations.

Skeletal and histological features of *Col2a1*^{Rgsc856} mutants

Col2a1^{Rgsc856} heterozygotes were mildly but significantly smaller than wild-type mice at E18.5 (Figs. 1a, b and 2). The limbs were disproportionately short (Fig. 2c), and the vertebral bodies were slightly hypoplastic (Fig. 2d). We generated *Col2a1*^{Rgsc856} homozygotes by crossing the heterozygotes. The homozygotes died at birth, exhibiting severe dwarfism with shortened limbs and a shortened snout (Fig. 2a, b). The skeletal specimens also showed a severe skeletal dysplasia, including extremely shortened limbs (Fig. 2c), severe spondylar dysplasia (Fig. 2d), severe pelvic hypoplasia (Fig. 2e), and brachydactyly (Fig. 2f). These defective skeletal features of the homozygotes are similar to those observed in PLSD-T patients.

To understand the pathogenic basis for the skeletal dysplasia phenotype, we investigated the histology of the

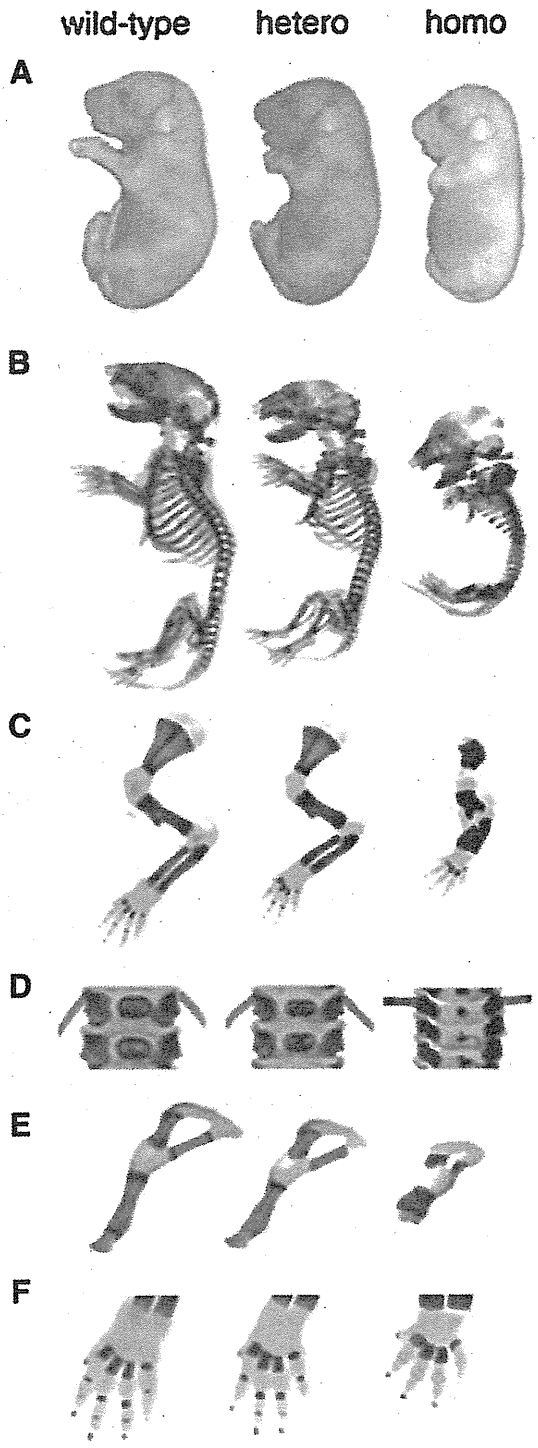

Fig. 2 Gross appearances and skeletal specimens of *Col2a1*^{Rgsc856} mutants at E18.5. **a** Gross appearances. **b–f** Skeletal specimens of whole skeleton (**b**), forelimb (**c**), lumbar spine (**d**), ilia (**e**), and forepaw (**f**). The homozygotes exhibited a severe skeletal dysplasia, including extremely shortened limbs, platyspondyly, severe pelvic hypoplasia, and brachydactyly

growth plate cartilage of *Col2a1*^{Rgsc856} mutants at E19.5 (Fig. 3). The growth plate of wild-type mice is composed of three distinct layers of chondrocytes—resting, proliferating, and hypertrophic zones—representing various stages of differentiation (Fig. 3A). Proliferating chondrocytes were well spaced by extracellular matrix (ECM) and exhibited typical columnar alignment with a flat shape (Fig. 3Ab). In the heterozygotes, this columnar alignment became disordered with reduced ECM spaces (Fig. 3Bb). In the homozygotes, the total length of the growth plate was drastically reduced but the diameter was increased (Fig. 3C). The columnar alignment of proliferating chondrocytes was completely lost (Fig. 3Cb), but hypertrophic chondrocytes were observed (Fig. 3Cc). The shape of the chondrocytes changed to a spindle-like cell in the resting and proliferating zones (Fig. 3Ca, Cb). Staining with toluidine blue, which binds to proteoglycans present in cartilage ECM, showed a drastic reduction in cartilage ECM in the proliferating zone of the homozygotes (Fig. 3D–F).

Characterization of molecular defects in the chondrocytes of *Col2a1*^{Rgsc856} mutants

We investigated the localization of type II collagen in the cartilage of *Col2a1*^{Rgsc856} mutants by immunohistochemical analysis using the sections from the proliferating zone of the femur at E19.5. In wild-type mice and the heterozygotes, immunoreactivity of type II collagen was observed mainly in the extracellular space of chondrocytes (Fig. 4a, b). In contrast, that in the homozygotes was scarcely detected in the extracellular space and was detected mainly in the intracellular space (Fig. 4c). Results of double staining with KDEL, an ER marker, suggested that a part of the mutant type II collagen was accumulating in the ER of chondrocytes in the homozygote (Fig. 4i).

We next performed an electron microscope analysis using samples from the proliferating zone of the femur at E18.5. In wild-type ECM, the collagen fibers showed dense and uniform distribution and many proteoglycan aggregations were found (Fig. 5a). The collagen fibers of the heterozygotes seemed to be slightly less dense (Fig. 5b), and those of the homozygotes were markedly reduced (Fig. 5c). Proteoglycan aggregates were also reduced and irregular in size in the homozygotes. Proliferating chondrocytes in wild-type mice contained well-developed organized rough ER (Fig. 5d). The rough ER was abnormally expanded in both the heterozygotes and the homozygotes (Fig. 5e, f). In the homozygotes, more expanded rough ER was evident compared to the heterozygotes.

Abnormally expanded rough ER and subsequent induction of ER stress have been reported in many mouse lines expressing mutant ECM proteins (Bateman et al. 2009). Expanded rough ER was also observed in mice lacking the ER stress sensor *Bbf2h7* (Saito et al. 2009). Therefore, we measured mRNA levels of two ER stress-related genes,

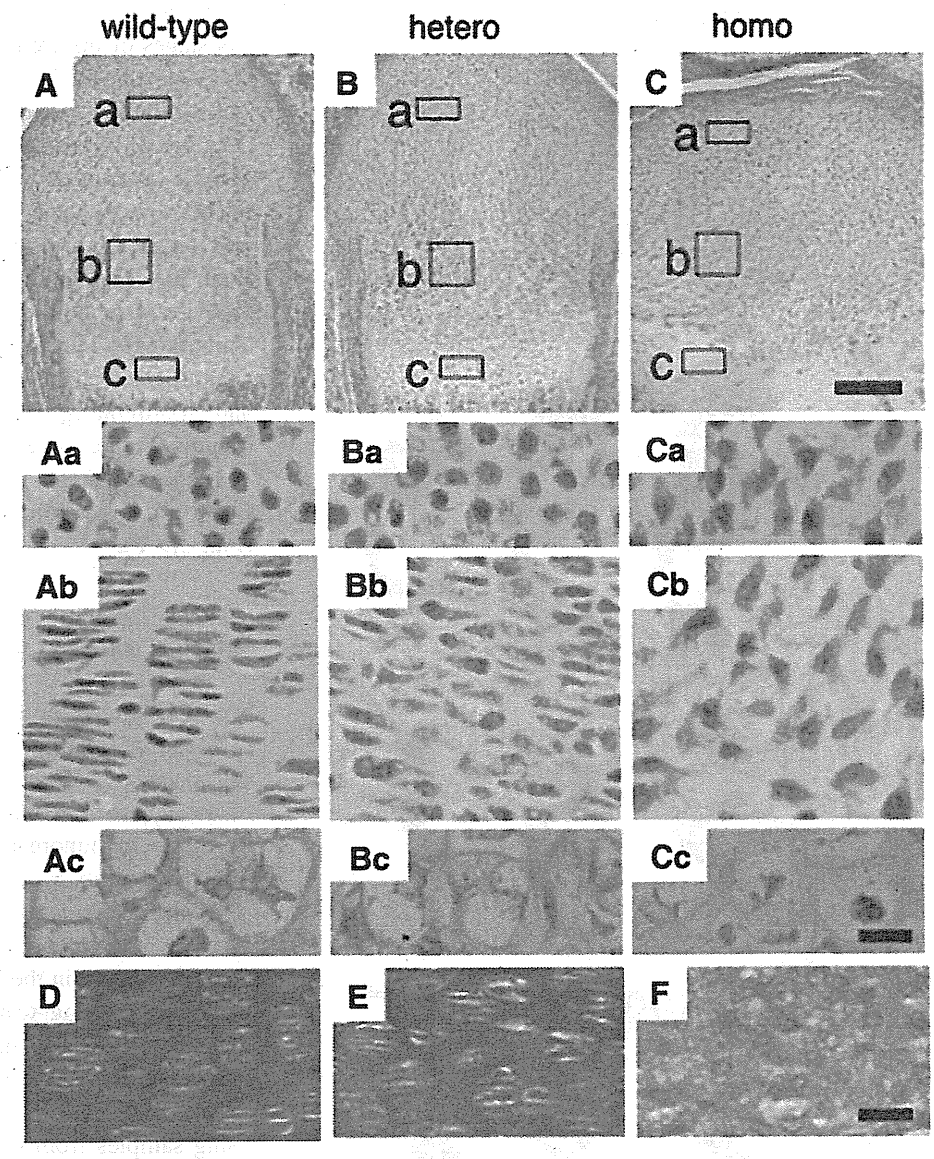

Fig. 3 Histology of growth plate cartilage from *Col2a1*^{Rgsc856} mutants at E19.5. **A–C** Hematoxylin & eosin (HE)–stained sections of the growth plate cartilage. The boxed regions (**a**, **b**, and **c**) represent the resting, proliferating, and hypertrophic zones, respectively. Magnified views of the boxed regions are shown in the same columns. **D–F** Toluidine blue-stained sections of the proliferating zone of the growth plate cartilage. Note that the total length of the growth plate cartilage was drastically reduced in the homozygotes (**C**). The typical columnar alignment of proliferating chondrocytes was observed in wild-type mice (**Ab**) but became disordered in the heterozygotes (**Bb**). This alignment was completely lost in the homozygotes (**Cb**). Weak staining by toluidine blue was evident in the homozygotes (**F**). *Scale bars* 50 μm (**A-C**) and 10 μm (**Aa–Cc** and **D–F**)

Grp94 and *Chop*, using rib cartilage samples at E18.5 (Fig. 6). GRP94 is an ER-resident chaperone, and CHOP is a transcription factor used as an ER stress marker (Bateman et al. 2009). Both genes are reported to be upregulated by ER stress. Their expression levels in both the heterozygotes and the homozygotes were significantly higher than those in wild-type mice, suggesting that ER stress was induced in *Col2a1*^{Rgsc856} mutants.

Osteoarthritis phenotypes in *Col2a1*^{Rgsc856} heterozygotes

Human diseases with *COL2A1* mutations are associated with early-onset OA (Loughlin 2001; Vikkula et al. 1993), and *Dmm* heterozygous mice develop early-onset OA that is conspicuous from 3 through 22 months of age (Bomsta et al. 2006). Therefore, we observed the histological appearance of the knee and elbow joints from wild-type mice and *Col2a1*^{Rgsc856} heterozygotes at 10 months of age. We stained the sections with safranin O (Fig. 7a) and evaluated OA severity with the modified Mankin scoring system (Fig. 7b). In both knee (Fig. 7) and elbow sections (data not shown), there were no significant differences in the score between wild-type and *Col2a1*^{Rgsc856} heterozygotes. In contrast to *Dmm* heterozygotes, *Col2a1*^{Rgsc856} heterozygotes did not show more severe degeneration of articular cartilage than wild-type mice at 10 months of age.

Discussion

Through phenotype-based screening in a large-scale ENU mutagenesis program, we identified a novel *Col2a1* mutant allele—*Col2a1*^{Rgsc856}. The mouse with *Col2a1*^{Rgsc856} is the second mutant with an endogenous C-propeptide mutation in *Col2a1* and the first animal model of PLSD-T. In the

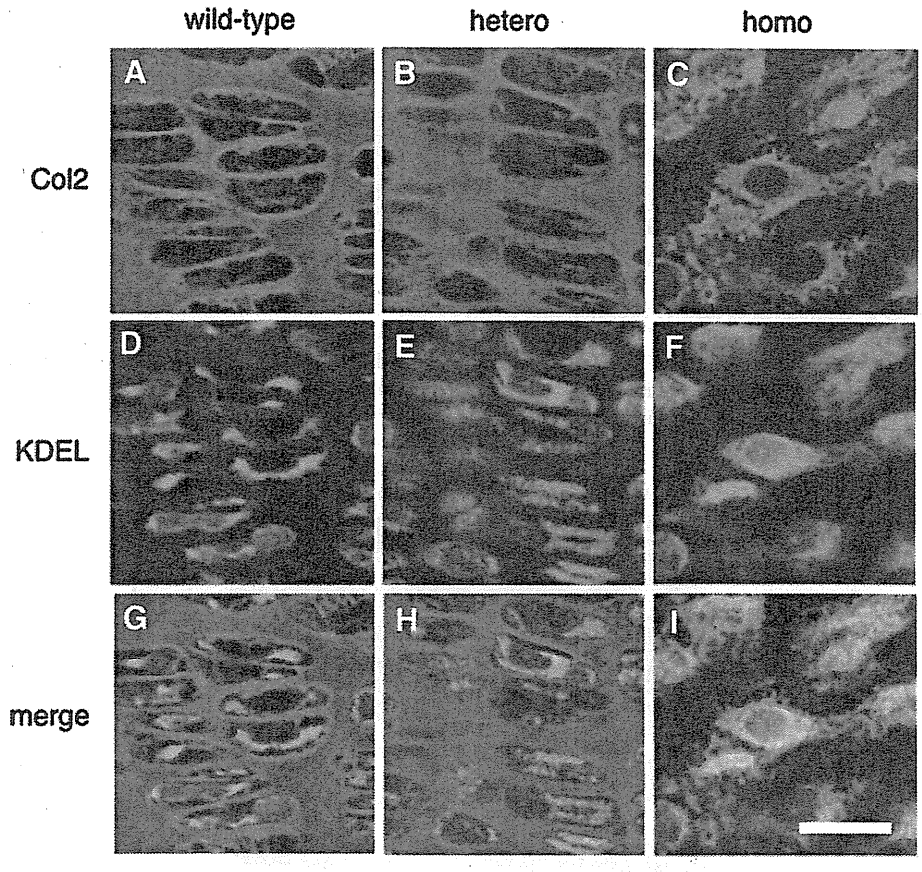

Fig. 4 Immunohistochemistry of type II collagen in the cartilage of *Col2a1*^{Rgsc856} mutants at E19.5. **a–c** The sections of the proliferating zone were stained with a type II collagen antibody. **d–f** Sections were stained with a KDEL (an ER marker) antibody. **g** Merge of **a** and **d**. **h** Merge of **b** and **e**. **i** Merge of **c** and **f**. Note that the immunoreactivity of type II collagen in wild-type mice (**a**) and the heterozygotes (**b**) was observed mainly in the extracellular space. In contrast, that in the homozygotes was in the intracellular space (**c**). *Scale bars* 10 μm

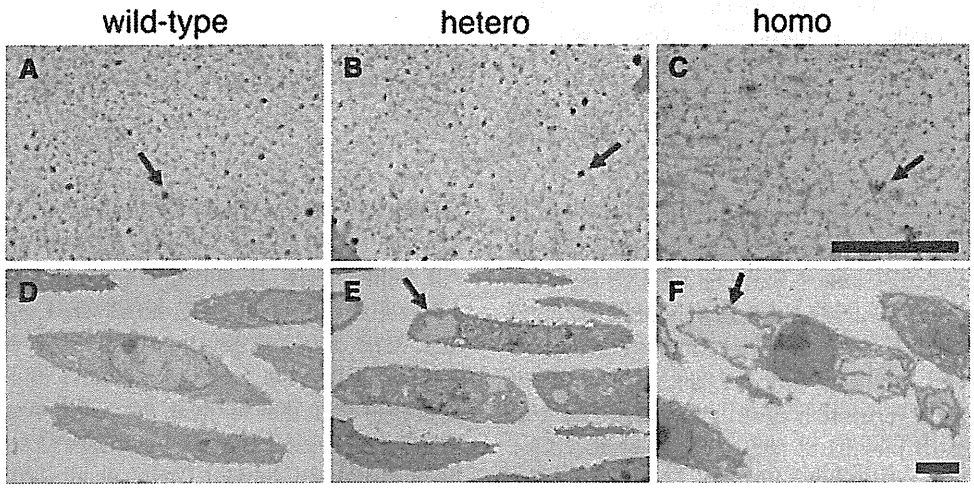

Fig. 5 Electron microscope images of the extracellular matrix (ECM) and chondrocytes from the proliferating zone in *Col2a1*^{Rgsc856} mutants at E18.5. **a–c** The images of the ECM are shown. *Arrows* indicate the proteoglycan aggregates. **d–f** The images of the chondrocytes are shown. *Arrows* show abnormally expanded rough endoplasmic reticulum (ER). Note that the collagen fibers of the homozygotes are markedly reduced (**c**). Abnormally expanded rough ER was found in the heterozygotes (**e**) and homozygotes (**f**). More expanded rough ER was evident in the homozygotes. *Scale bars* 1 μm (**a–c**) and 2 μm (**d–f**)

chondrocytes of *Col2a1*^{Rgsc856} mutants, secretion of mutant type II collagens into the extracellular space is disrupted, accompanied by abnormally expanded ER and upregulation of ER stress-related genes. These findings strongly suggested that ER stress is induced in the mutants.

Two mouse lines possessing an endogenous *Col2a1* mutation have been established. Until now, the *Dmm* mouse was the only known animal model with an endogenous C-propeptide mutation in *Col2a1* (Brown et al. 1981; Pace et al. 1997). Although the substituted amino acid in

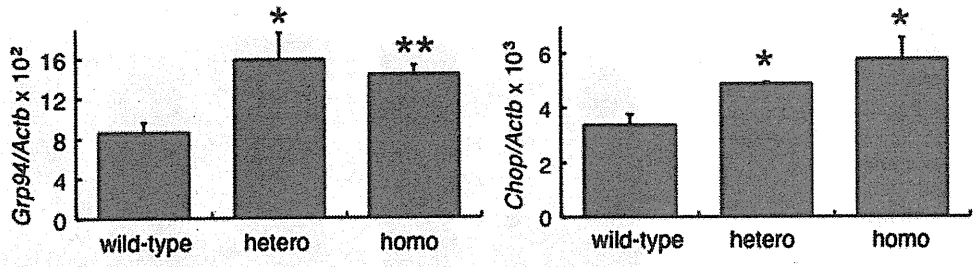

Fig. 6 Expression of mRNA encoding ER stress-related molecules in the rib cartilages of $Col2a1^{Rgsc856}$ mutants at E18.5. GRP94 is an ER-resident chaperone and CHOP is a transcription factor used as an ER stress marker. Data were normalized with the expression levels of *Actb*. Data are expressed as the mean ± SE ($n = 5$). The p value was determined by one-way ANOVA followed by Bonferroni's test. * $p < 0.05$, ** $p < 0.01$. The same result was obtained from the independent experiment conducted using E19.5 embryos. The expression levels of the two genes in $Col2a1^{Rgsc856}$ mutants were significantly higher than those in wild-type mice

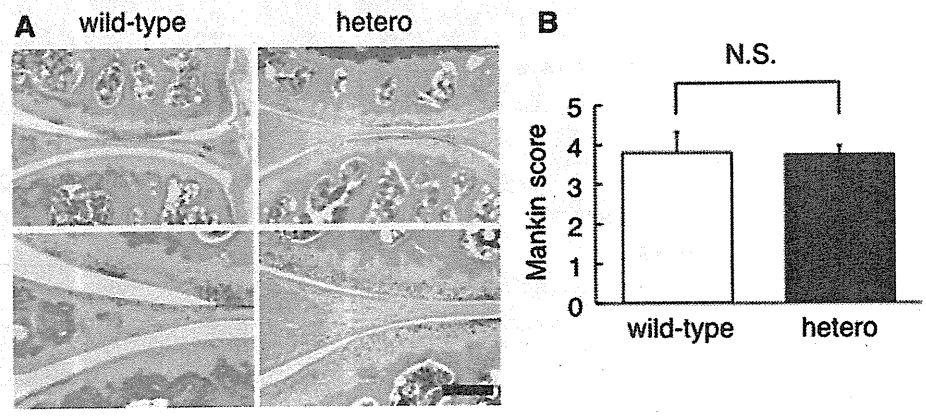

Fig. 7 Histological and histochemical evaluation (modified Mankin score) of articular cartilage in $Col2a1^{Rgsc856}$ heterozygotes at 10 months of age. **a** Sections of the knee joint were stained with safranin O. **b** Modified Mankin score using the sections of knee joint. Data are expressed as the mean ± SE [wild type: $n = 5$ (two males and three females), $Col2a1^{Rgsc856}$ heterozygous: $n = 4$ (two males and three females)]. The p value was determined by the Mann-Whitney U test. There was no significant difference between wild-type mice and $Col2a1^{Rgsc856}$ heterozygotes. The same result was obtained in the analysis using sections from the elbow joint. *Scale bar* 100 μm

$Col2a1^{Rgsc856}$ mutants (D1469) is located close to that in *Dmm* mice (K1448_T1449) in the C-propeptide region, there are phenotypic differences between the two mutants. At the newborn stage, the body size of *Dmm* heterozygotes is normal, but $Col2a1^{Rgsc856}$ heterozygotes were significantly smaller than wild-type mice. *Dmm* heterozygotes show more severe degeneration of articular cartilage than wild-type mice at 10 months of age (Bomsta et al. 2006), but $Col2a1^{Rgsc856}$ heterozygotes did not. Detailed phenotypic distinction between the two mutants is required. On the other hand, *Sedc* mice, a spontaneous mutant, carry a *Col2a1* missense mutation (c.3574C>T, p.R1192C) located near the C-terminus of the triple-helical domain (Donahue et al. 2003). Because this mutation causes the same amino acid substitution in SEDC patients, the mutant allele was named as *Sedc*. *Sedc* homozygotes are smaller than wild-type mice but can survive to adulthood and be fertile. Adult *Sedc* homozygotes exhibit mild skeletal dysplasia, retinoschisis, and hearing loss. *Sedc* mutants offer a valuable model to examine SEDC pathogenesis and the effect of mutations that substitute the amino acid residue in the X position of the Gly-X-Y repeat in the triple-helical domain. All human type II collagenopathies are inherited as an autosomal dominant trait; however, $Col2a1^{Rgsc856}$, *Dmm*, and *Sedc* heterozygotes exhibit very mild phenotypes, indicating that the effect of *COL2A1* mutations in humans is greater than that in mice. Several transgenic mouse lines that overexpress various mutant type II collagen molecules have also been studied (Arita et al. 2002; Maddox et al. 1997; Metsaranta et al. 1992). Because the large amount of mutant proteins from transgenes generally results in strong dominant-negative effects, most transgenic mouse lines exhibit embryonic lethality.

PLSD-T is a rare skeletal dysplasia characterized by platyspondyly, extremely short limbs, severe pelvic hypoplasia, and mild brachydactyly (Nishimura et al. 2004; Zankl et al. 2005). This disease is caused by heterozygous *COL2A1* mutations in the C-propeptide coding region and is generally lethal in the perinatal period, although a few long-term survivors have been reported. Because

of a number of phenotypic similarities, *Col2a1*^{Rgsc856} homozygotes offer a better model to examine PLSD-T pathogenesis. Indeed, the homozygotes showed skeletal features similar to those of PLSD-T patients. Furthermore, abnormally expanded rough ER was observed in both *Col2a1*^{Rgsc856} homozygotes and PLSD-T patients (Freisinger et al. 1996; Zankl et al. 2005). Our results from immunohistochemistry and electron microscope analyses indicated that in the homozygotes, mutant type II collagens accumulated in the expanded rough ER of chondrocytes and were poorly secreted into the extracellular space. The upregulation of ER stress-related genes (*Grp94* and *Chop*) suggested that ER stress was induced in *Col2a1*^{Rgsc856} mutants. These defects may disrupt the ECM network and zonal structure of growth plate cartilage and lead to severe skeletal dysplasia. The same molecular events may occur in PLSD-T pathogenesis.

The C-propeptide of fibrillar collagen plays a crucial role in triple-helical formation (Doege and Fessler 1986; Khoshnoodi et al. 2006). Once procollagen chains translocate into the lumen of the ER, they associate via their C-propeptides to form a trimer. This initial association is stabilized by intra- and interchain disulfide bonds. Triple-helix formation then occurs from the carboxyl- to the amino-terminal end. Intracellular accumulation of mutant proteins was observed in *Col2a1*^{Rgsc856} homozygotes, and an abnormally expanded ER was observed in both the homozygotes and the heterozygotes. These results indicated that the D1469 residue substituted in the *Col2a1*^{Rgsc856} allele is essential for the function of the C-propeptide. Intracellular accumulation of mutant proteins seems to be common to both *Col2a1*^{Rgsc856} and *Dmm* mutants (Fernandes et al. 2003; Seegmiller et al. 2008). Mutations in the *Col2a1*^{Rgsc856} and *Dmm* alleles are located close to each other, between the last two cysteine residues involved in the formation of intrachain disulfide bonds. The amino acid substitution in the *Dmm* allele (p.K1448_T1449delinsN) is predicted to change the local secondary structure from coil to strand (Fernandes et al. 2003). On the other hand, the substitution in the *Col2a1*^{Rgsc856} allele (p.D1469A) is predicted to cause a drastic polarity change. These varied effects may generate the phenotypic differences between the two mutants. C-propeptide is also known as chondrocalcin, which accumulates in the ECM of the hypertrophic zone of growth plate cartilage and seems to promote mineralization (Van der Rest et al. 1986); however, little else is known about this protein. *Col2a1*^{Rgsc856} mutants may also be useful to investigate C-propeptide functions as chondrocalcin.

Accumulation of misfolded mutant proteins in the ER induces ER stress (Ron and Walter 2007; Schroder and Kaufman 2005). In response to ER stress, eukaryotic cells increase transcription of genes encoding ER-resident chaperones such as BiP/GRP78 and GRP94; this system is termed the unfolded protein response (UPR). CHOP is a UPR-induced transcription factor used as an ER stress marker. The UPR is initially a response to relieve ER stress but if unresolved, it can lead to apoptotic cell death. Recently, misfolded mutant ECM proteins such as collagens, COMP, and matrilin 3 have been shown to induce ER stress and UPR (Bateman et al. 2009). It has been reported that the type I procollagen chains with the C-propeptide mutations identified in patients with osteogenesis imperfecta bind to BiP and upregulate the expression of both BiP and GRP94 (Chessler and Byers 1993). Type X procollagen chains with C-terminal noncollagenous (NC1) domain mutations identified in patients with metaphyseal chondrodysplasia (Schmid type) are unable to assemble into homotrimers and perform extracellular secretion (Wilson et al. 2005). These mutants have upregulated BiP and a spliced form of mRNA of the X-box binding protein 1 (*XBP1*), another key marker for the UPR. Activation of the UPR has been confirmed in transgenic mice expressing type X collagen with a 13-bp deletion within the NC1 domain (Tsang et al. 2007). Type II collagen chains with a triple-helical mutation—p.R989C—identified in SEDC patients upregulate and bind to BiP (Hintze et al. 2008). Furthermore, cells overexpressing the p.R989C mutant undergo apoptosis. It has also been reported that BiP and CHOP are upregulated in *Col2a1* transgenic mice expressing the triple-helical mutant p.G904C (Tsang et al. 2007). We demonstrated that *Grp94* and *Chop* expression was upregulated in *Col2a1*^{Rgsc856} mutants, suggesting that ER stress and the UPR is also induced in PLSD-T patients. It should be elucidated how the UPR and its downstream consequences, such as apoptosis and altered gene expression, relate to PLSD-T pathogenesis.

OA is the most common joint disease characterized by progressive degeneration of articular cartilage. *COL2A1* mutations have been identified in various types of skeletal dysplasias, some of which include OA in their phenotype (Loughlin 2001; Vikkula et al. 1993). Several studies suggest an association of *COL2A1* polymorphisms with OA (Ikeda et al. 2002). *Dmm* heterozygotes develop premature OA that is conspicuous from 3 through 22 months of age (Bomsta et al. 2006). In contrast, *Col2a1*^{Rgsc856} heterozygotes did not show a more severe degeneration of articular cartilage than wild-type mice at 10 months of age. Therefore, the *Dmm* allele should make a larger contribution to the OA phenotype than the *Col2a1*^{Rgsc856} allele. Combinational use of *Dmm* and *Col2a1*^{Rgsc856} heterozygotes may lead to an understanding of the relationship between the functional defect of the C-propeptide and the development of OA.

We have described skeletal and histological features of *Col2a1*^{Rgsc856} mutant mice that should become useful as a model of PLSD-T. Collection of more mutant alleles of

Col2a1 would lead to a better understanding of the mechanisms responsible for creating the great diversity of type II collagenopathies.

Acknowledgments We are grateful to Dr. S. Tominaga, Mrs. H. Yokoyama, and J. Nagano for their help with managing the animals, preparation of samples, identification of the mutation, and mouse genotyping. We also thank Charles River Laboratories Japan, Inc. for help with mouse breeding. This project was supported by grants-in-aid from the Ministry of Education, Culture, Sports and Science of Japan (contract grant Nos. 20390408 and 21249080), Research on Child Health and Development (contract grant No. 20-S-3), and Naito Foundation.

References

Ahmad NN, Ala-Kokko L, Knowlton RG, Jimenez SA, Weaver EJ, Maguire JI, Tasman W, Prockop DJ (1991) Stop codon in the procollagen II gene (*COL2A1*) in a family with the Stickler syndrome (arthro-ophthalmopathy). Proc Natl Acad Sci USA 88:6624–6627

Arita M, Li SW, Kopen G, Adachi E, Jimenez SA, Fertala A (2002) Skeletal abnormalities and ultrastructural changes of cartilage in transgenic mice expressing a collagen II gene (COL2A1) with a Cys for Arg-alpha1–519 substitution. Osteoarthr Cartil 10:808–815

Bateman JF, Boot-Handford RP, Lamande SR (2009) Genetic diseases of connective tissues: cellular and extracellular effects of ECM mutations. Nat Rev Genet 10:173–183

Bomsta BD, Bridgewater LC, Seegmiller RE (2006) Premature osteoarthritis in the Disproportionate micromelia (*Dmm*) mouse. Osteoarthr Cartil 14:477–485

Brown KS, Cranley RE, Greene R, Kleinman HK, Pennypacker JP (1981) Disproportionate micromelia (*Dmm*): an incomplete dominant mouse dwarfism with abnormal cartilage matrix. J Embryol Exp Morphol 62:165–182

Chessler SD, Byers PH (1993) BiP binds type I procollagen pro alpha chains with mutations in the carboxyl-terminal propeptide synthesized by cells from patients with osteogenesis imperfecta. J Biol Chem 268:18226–18233

Doege KJ, Fessler JH (1986) Folding of carboxyl domain and assembly of procollagen I. J Biol Chem 261:8924–8935

Donahue LR, Chang B, Mohan S, Miyakoshi N, Wergedal JE, Baylink DJ, Hawes NL, Rosen CJ, Ward-Bailey P, Zheng QY, Bronson RT, Johnson KR, Davisson MT (2003) A missense mutation in the mouse *Col2a1* gene causes spondyloepiphyseal dysplasia congenita, hearing loss, and retinoschisis. J Bone Miner Res 18:1612–1621

Fernandes RJ, Seegmiller RE, Nelson WR, Eyre DR (2003) Protein consequences of the *Col2a1* C-propeptide mutation in the chondrodysplastic *Dmm* mouse. Matrix Biol 22:449–453

Freisinger P, Bonaventure J, Stoess H, Pontz BF, Emmrich P, Nerlich A (1996) Type II collagenopathies: are there additional family members? Am J Med Genet 63:137–143

Hintze V, Steplewski A, Ito H, Jensen DA, Rodeck U, Fertala A (2008) Cells expressing partially unfolded R789C/p.R989C type II procollagen mutant associated with spondyloepiphyseal dysplasia undergo apoptosis. Hum Mutat 29:841–851

Hitotsumachi S, Carpenter DA, Russell WL (1985) Dose-repetition increases the mutagenic effectiveness of *N*-ethyl-*N*-nitrosourea in mouse spermatogonia. Proc Natl Acad Sci USA 82:6619–6621

Ikeda T, Mabuchi A, Fukuda A, Kawakami A, Ryo Y, Yamamoto S, Miyoshi K, Haga N, Hiraoka H, Takatori Y, Kawaguchi H, Nakamura K, Ikegawa S (2002) Association analysis of single nucleotide polymorphisms in cartilage-specific collagen genes with knee and hip osteoarthritis in the Japanese population. J Bone Miner Res 17:1290–1296

Inoue M, Sakuraba Y, Motegi H, Kubota N, Toki H, Matsui J, Toyoda Y, Miwa I, Terauchi Y, Kadowaki T, Shigeyama Y, Kasuga M, Adachi T, Fujimoto N, Matsumoto R, Tsuchihashi K, Kagami T, Inoue A, Kaneda H, Ishijima J, Masuya H, Suzuki T, Wakana S, Gondo Y, Minowa O, Shiroishi T, Noda T (2004) A series of maturity onset diabetes of the young, type 2 (MODY2) mouse models generated by a large-scale ENU mutagenesis program. Hum Mol Genet 13:1147–1157

Khoshnoodi J, Cartailler JP, Alvares K, Veis A, Hudson BG (2006) Molecular recognition in the assembly of collagens: terminal noncollagenous domains are key recognition modules in the formation of triple helical protomers. J Biol Chem 281: 38117–38121

Korkko J, Cohn DH, Ala-Kokko L, Krakow D, Prockop DJ (2000) Widely distributed mutations in the *COL2A1* gene produce achondrogenesis type II/hypochondrogenesis. Am J Med Genet 92:95–100

Kuivaniemi H, Tromp G, Prockop DJ (1997) Mutations in fibrillar collagens (types I, II, III, and XI), fibril-associated collagen (type IX), and network-forming collagen (type X) cause a spectrum of diseases of bone, cartilage, and blood vessels. Hum Mutat 9:300–315

Li SW, Prockop DJ, Helminen H, Fassler R, Lapvetelainen T, Kiraly K, Peltarri A, Arokoski J, Lui H, Arita M et al (1995) Transgenic mice with targeted inactivation of the *Col2a1* gene for collagen II develop a skeleton with membranous and periosteal bone but no endochondral bone. Genes Dev 9:2821–2830

Loughlin J (2001) Genetic epidemiology of primary osteoarthritis. Curr Opin Rheumatol 13:111–116

Maddox BK, Garofalo S, Smith C, Keene DR, Horton WA (1997) Skeletal development in transgenic mice expressing a mutation at Gly574Ser of type II collagen. Dev Dyn 208:170–177

Mankin HJ, Dorfman H, Lippiello L, Zarins A (1971) Biochemical and metabolic abnormalities in articular cartilage from osteoarthritic human hips. II. Correlation of morphology with biochemical and metabolic data. J Bone Joint Surg Am 53: 523–537

Masuya H, Inoue M, Wada Y, Shimizu A, Nagano J, Kawai A, Inoue A, Kagami T, Hirayama T, Yamaga A, Kaneda H, Kobayashi K, Minowa O, Miura I, Gondo Y, Noda T, Wakana S, Shiroishi T (2005a) Implementation of the modified-SHIRPA protocol for screening of dominant phenotypes in a large-scale ENU mutagenesis program. Mamm Genome 16:829–837

Masuya H, Shimizu K, Sezutsu H, Sakuraba Y, Nagano J, Shimizu A, Fujimoto N, Kawai A, Miura I, Kaneda H, Kobayashi K, Ishijima J, Maeda T, Gondo Y, Noda T, Wakana S, Shiroishi T (2005b) Enamelin (*Enam*) is essential for amelogenesis: ENU-induced mouse mutants as models for different clinical subtypes of human amelogenesis imperfecta (AI). Hum Mol Genet 14: 575–583

Masuya H, Nishida K, Furuichi T, Toki H, Nishimura G, Kawabata H, Yokoyama H, Yoshida A, Tominaga S, Nagano J, Shimizu A, Wakana S, Gondo Y, Noda T, Shiroishi T, Ikegawa S (2007) A novel dominant-negative mutation in *Gdf5* generated by ENU mutagenesis impairs joint formation and causes osteoarthritis in mice. Hum Mol Genet 16:2366–2375

Metsaranta M, Garofalo S, Decker G, Rintala M, de Crombrugghe B, Vuorio E (1992) Chondrodysplasia in transgenic mice harboring a 15-amino-acid deletion in the triple helical domain of pro alpha 1(II) collagen chain. J Cell Biol 118:203–212

Mortier GR, Weis M, Nuytinck L, King LM, Wilkin DJ, De Paepe A, Lachman RS, Rimoin DL, Eyre DR, Cohn DH (2000) Report of five novel and one recurrent *COL2A1* mutation with analysis of genotype-phenotype correlation in patients with a lethal type II collagen disorder. J Med Genet 37:263–271

Myllyharju J, Kivirikko KI (2004) Collagens, modifying enzymes and their mutations in humans, flies and worms. Trends Genet 20:33–43

Nishimura G, Nakashima E, Mabuchi A, Shimamoto K, Shimamoto T, Shimao Y, Nagai T, Yamaguchi T, Kosaki R, Ohashi H, Makita Y, Ikegawa S (2004) Identification of *COL2A1* mutations in platyspondylic skeletal dysplasia, Torrance type. J Med Genet 41:75–79

Nishimura G, Haga N, Kitoh H, Tanaka Y, Sonoda T, Kitamura M, Shirahama S, Itoh T, Nakashima E, Ohashi H, Ikegawa S (2005) The phenotypic spectrum of *COL2A1* mutations. Hum Mutat 26:36–43

Nolan PM, Kapfhamer D, Bucan M (1997) Random mutagenesis screen for dominant behavioral mutations in mice. Methods 13:379–395

Olsen BR (1995) New insights into the function of collagens from genetic analysis. Curr Opin Cell Biol 7:720–727

Pace JM, Li Y, Seegmiller RE, Teuscher C, Taylor BA, Olsen BR (1997) Disproportionate micromelia (Dmm) in mice caused by a mutation in the C-propeptide coding region of *Col2a1*. Dev Dyn 208:25–33

Ron D, Walter P (2007) Signal integration in the endoplasmic reticulum unfolded protein response. Nat Rev Mol Cell Biol 8:519–529

Saito A, Hino S, Murakami T, Kanemoto S, Kondo S, Saitoh M, Nishimura R, Yoneda T, Furuichi T, Ikegawa S, Ikawa M, Okabe M, Imaizumi K (2009) Regulation of endoplasmic reticulum stress response by a BBF2H7-mediated Sec23a pathway is essential for chondrogenesis. Nat Cell Biol 11: 1197–1204

Schroder M, Kaufman RJ (2005) ER stress and the unfolded protein response. Mutat Res 569:29–63

Seegmiller RE, Bomsta BD, Bridgewater LC, Niederhauser CM, CMontaño C, Sudweeks S, Eyre DR, Fernandes RJ (2008) The heterozygous disproportionate micromelia (*Dmm*) mouse: morphological changes in fetal cartilage precede postnatal dwarfism and compared with lethal homozygotes can explain the mild phenotype. J Histochem Cytochem 56:1003–1011

Tsang KY, Chan D, Cheslett D, Chan WC, So CL, Melhado IG, Chan TW, Kwan KM, Hunziker EB, Yamada Y, Bateman JF, Cheung KM, Cheah KS (2007) Surviving endoplasmic reticulum stress is coupled to altered chondrocyte differentiation and function. PLoS Biol 5:e44

Unger S, Korkko J, Krakow D, Lachman RS, Rimoin DL, Cohn DH (2001) Double heterozygosity for pseudoachondroplasia and spondyloepiphyseal dysplasia congenita. Am J Med Genet 104: 140–146

Van der Rest M, Rosenberg LC, Olsen BR, Poole AR (1986) Chondrocalcin is identical with the C-propeptide of type II procollagen. Biochem J 237:923–925

van der Sluijs JA, Geesink RG, van der Linden AJ, Bulstra SK, Kuyer R, Drukker J (1992) The reliability of the Mankin score for osteoarthritis. J Orthop Res 10:58–61

Vikkula M, Palotie A, Ritvaniemi P, Ott J, Ala-Kokko L, Sievers U, Aho K, Peltonen L (1993) Early-onset osteoarthritis linked to the type II procollagen gene. Detailed clinical phenotype and further analyses of the gene. Arthritis Rheum 36:401–409

Wilson R, Freddi S, Chan D, Cheah KS, Bateman JF (2005) Misfolding of collagen X chains harboring Schmid metaphyseal chondrodysplasia mutations results in aberrant disulfide bond formation, intracellular retention, and activation of the unfolded protein response. J Biol Chem 280:15544–15552

Winterpacht A, Hilbert M, Schwarze U, Mundlos S, Spranger J, Zabel BU (1993) Kniest and Stickler dysplasia phenotypes caused by collagen type II gene (*COL2A1*) defect. Nat Genet 3:323–326

Zabel B, Hilbert K, Stoss H, Superti-Furga A, Spranger J, Winterpacht A (1996) A specific collagen type II gene (*COL2A1*) mutation presenting as spondyloperipheral dysplasia. Am J Med Genet 63:123–128

Zankl A, Neumann L, Ignatius J, Nikkels P, Schrander-Stumpel C, Mortier G, Omran H, Wright M, Hilbert K, Bonafe L, Spranger J, Zabel B, Superti-Furga A (2005) Dominant negative mutations in the C-propeptide of *COL2A1* cause platyspondylic lethal skeletal dysplasia, torrance type, and define a novel subfamily within the type 2 collagenopathies. Am J Med Genet A 133A:61–66

PSYCHOGERIATRICS
The Official Journal of the Japanese Psychogeriatric Society

doi:10.1111/j.1479-8301.2011.00355.x PSYCHOGERIATRICS 2011; 11: 90–97

ORIGINAL ARTICLE

Protein kinase C stabilizes X-linked inhibitor of apoptosis protein (XIAP) through phosphorylation at Ser^{87} to suppress apoptotic cell death

Kiyoko KATO,[1] Toshihisa TANAKA,[1] Golam SADIK,[2] Miyako BABA,[1] Daisuke MARUYAMA,[1] Kanta YANAGIDA,[1] Takashi KODAMA,[1] Takashi MORIHARA,[1] Shinji TAGAMI,[1] Masayasu OKOCHI,[1] Takashi KUDO[1] and Masatoshi TAKEDA[1]

[1]Department of Psychiatry, Osaka University Graduate School of Medicine, Osaka, Japan and [2]Department of Pharmacy, University of Rajshahi, Rajshahi, Bangladesh

Correspondence: Dr. Toshihisa Tanaka, MD, PhD, Department of Psychiatry, Osaka University Graduate School of Medicine, D3, 2-2, Yamadaoka, Suita, Osaka 565-0871, Japan. E-mail: tanaka@psy.med.osaka-u.ac.jp

Received 22 December 2010; accepted 13 January 2011.

Abstract

Background: Multiple protein kinases have been shown to be involved in the apoptotic neuronal loss of Alzheimer's disease (AD). Although some studies support the role of protein kinase C (PKC) in amyloid precursor protein processing as well as in tau phosphorylation, a direct role for PKC in apoptotic neuronal death remains to be clarified. In the present study, we report on the possible role of PKC in cell survival during conditions of stress through phosphorylation of the X-linked inhibitor of apoptosis protein (XIAP).

Methods: Phosphorylation of XIAP at Ser87 was confirmed by western blot analysis employing phosphorylation dependent anti-XIAP antibody after incubation of recombinant XIAP with active PKC *in vitro*. And increased phosphorylation of XIAP at the site was also confirmed in SH-SY5Y cells treated with PKC activator, phorbol 12-myristate 13-acetate (PMA). A mutant XIAP construct in which Ser87 was substituted by Ala, was prepared, and transfected to cells. After the transfection of wild or mutant XIAP, cells viability was evaluated by counting living and dead cells treated with PMA during etoposide-induced apoptosis.

Results: Recombinant XIAP was phosphorylated at Ser^{87} by PKC *in vitro* and treatment of XIAP-transfected SH-SY5Y cells with a PKC activator, phorbol 12-myristate 13-acetate (PMA) induced phosphorylation of XIAP at Ser^{87}. Pulse chase experiments revealed that, when phosphorylated at Ser^{87}, wild-type XIAP is more stable than XIAP with a Ser87Ala substitution, which is degraded faster. Importantly, the phosphorylation of XIAP at the site by PKC significantly increased cell survival up to approximately 2.5 times under the condition of apoptosis induced by 25 μg/ml etoposide.

Conclusion: The findings of the present study indicate a role for PKC, through phosphorylation of XIAP at Ser^{87} and its stabilization, in cell survival under conditions of stress and lend strength to the idea that PKC is crucial in regulating neuronal homeostasis, which may be impaired in AD.

Key words: *apoptosis, neuronal cell, neuroprotection, phosphorylation, protein kinase C, X-linked inhibitor of apoptosis protein.*

INTRODUCTION

In neurodegenerative diseases, such as Alzheimer's disease (AD), neuronal loss is, in large part, the consequence of the activation of apoptotic cascades and changes in both apoptotic and anti-apoptotic factors have been reported.[1] Inhibitors of apoptosis proteins (IAPs) are endogenous anti-apoptosis regulators and, to date, eight IAPs have been

identified in humans (neuronal apoptosis inhibitor protein [NAIP], cellular-inhibitor of apoptosis of protein [c-IAP]1/human inhibitor of apoptosis protein [HIAP]-2, c-IAP2/HIAP-1, X-linked inhibitor of apoptosis protein (XIAP)/human IAP-like protein [hILP]-1, hILP-2/testis specific inhibitor of apoptosis protein [Ts-IAP], Survivin, melanoma-inhibitor of apoptosis protein [ML-IAP]/Livin, and Apollon/Bruce).[2–7] Of these IAPs, XIAP is the most potent inhibitor of apoptosis and it suppresses apoptosis by inhibiting the activation of caspases-3, -7. and -9.[8–10] We have reported previously that the expression of XIAP in SH-SY5Y cells is significantly reduced in a concentration-dependent manner when the cells are exposed to low concentrations of β-amyloid.[11]

It has been shown that phosphorylation of XIAP by protein kinase (PK) B reduces XIAP ubiquitination and degradation, and that increased levels of XIAP are associated with protection against cisplatin-stimulated apoptosis in A2780S ovarian cancer cells.[12] However, PKC is one of the most abundant cellular protein kinases and it is found in high levels in the brain. In addition, decreased levels of PKC and a reduction in the phosphorylation of PKC substrates are biochemical characteristics of AD post-mortem brain tissue,[13–16] suggesting that dysregulation of PKC activity may represent a crucial step in the pathology of AD. Importantly, it has been demonstrated that XIAP is ubiquitinated and degraded when PKC activation is suppressed.[17] However, whether PKC has a neuroprotective effect by stabilizing XIAP through its phosphorylation, which could be severely impaired in AD, is not known. Thus, we hypothesized that phosphorylation of XIAP by PKC is an important physiological mechanism for cell survival under stress conditions and that regulation of PKC activity may be central in neurodegenerative processes by modulating XIAP stability. Here, we show that XIAP is directly phosphorylated by PKC and that XIAP phosphorylated at Ser^{87} by PKC is resistant to degradation, protecting SH-SY5Y cells from apoptosis-inducing stress.

METHODS

Antibodies

The following antibodies were used in the present study: anti-hILP/XIAP (BD Bioscience, San Jose, CA, USA), anti-phosphorylated (p-) Ser^{87} XIAP (Abcam, Cambridge, MA, USA), and anti-C-terminus XIAP (ProSci, Poway, CA, USA).

Plasmid construct and cell culture

The XIAP gene, a generous gift from Dr J. D. Ashwell (National Institutes of Health, Bethesda, MD, USA), was cut with *BamH*I and *Not*I restriction enzymes and inserted with a linker into the pcDNA3.1(+) vector (Invitrogen, Carsbad, CA, USA) after cutting with *Nhe*I and *Xho*I. The XIAP-Ser87A mutant construct was generated by cloning in the oligonucleotides 5′-gaaagtagccccaaattgcaga-3′ and 3′-tctgcaatttggggct actttc-5′ using a QuikChange II XL Site-Directed Mutagenesis Kit (Stratagene, La Jolla, CA, USA) according to the manufacturer's instructions.

SH-SY5Y neuroblastoma cells, a kind gift from Dr J. L. Biedler (Sloan Kettering Institute, New York, NY, USA), were cultured in Dulbecco's modified Eagle's medium (DMEM)/F12 medium (Gibco, Carlsbad, CA, USA) with 10% fetal bovine serum (JRH, Lenexa, KA, USA) and 10 units/mL penicillin plus 10 μg/mL streptomycin (Gibco) at 37°C under 5% CO_2. Cells were transfected with the appropriate DNA, using Lipofectamine LTX (Invitrogen) according to the manufacturer's instructions. Stably transfected cells were selected and maintained in selective medium supplemented with 400 μg/mL G418 (Invitrogen).

Phosphorylation of recombinant XIAP *in vitro*

The XIAP gene was cut with *BamH*I and *Xho*I restriction enzymes and inserted with a linker into the pET-22b(+) vector (Novagen, Darmastadt, Germany). The XIAP-harboring pET-22b was transformed into *Escherichia coli* BL21 (DE3) for expression of recombinant XIAP. *In vitro* phosphorylation of XIAP by PKB and PKC was achieved by incubating XIAP (0.5 μg/μL) for 2 h at 37°C with the following reaction mixtures: (i) for PKB, 40 ng/μL active Akt1/PKBα (Upstate, Laka Placid, NY, USA; 30 mmol/L Tris, pH 7.4, 10 mmol/L $MgCl_2$, 10 mmol/L NaF, 1 mmol/L Na_3VO_4, 2 mmol/L EGTA, 10 mmol/L β-mercaptoethanol, 0.2 mmol/L ATP, 4 mmol/L dithiothreitol); (ii) for PKC, 6 ng/μL active PKC (Sigma, St Louis, MO, USA; ADBII Buffer (Millipore, Billerica, MA, USA), 0.2 mmol/L ATP, 71 μg/mL PKC Lipid Activator (Millipore), 10 mmol/L $MgCl_2$). To terminate enzymatic reactions, samples were boiled with an equal volume of sodium dodecyl sulfate (SDS) sample buffer for 5 min.

Immunoprecipitation and western blot analysis

To activate PKC, SH-SY5Y cells stably transfected with wild-type XIAP were treated with 100 nmol/L Phorbol myristate acetate (PMA; Sigma) for 6 h. The treated cells were scraped in lysis buffer (50 mmol/L Tris-HCl (pH 7.3), 150 mmol/L NaCl, 1% TritonX-100, 1 mmol/L EGTA, 0.1% SDS, supplemented with phosphatase inhibitor cocktail (Thermo Scientific, Rockford, IL, USA), protease inhibitor cocktail (Sigma), and 1 mmol/L benzylsulfonyl fluoride (Wako, Osaka, Japan)) and then left on ice for 30 min. The supernatant was collected after centrifugation at 20 000 *g* for 15 min. Protein concentrations were determined using the bicinchoninic acid assay (BCA; Thermo Scientific). Anti-XIAP antibody (2 μg) was added to 1.5 mg lysate and mixtures were rotated overnight at 4°C. Protein G agarose beads were added (GE Healthcare, Tokyo, Japan), followed by rotation for 1.5 h at 4°C. The beads were washed four times using ice-cold Tris-buffered saline (TBS) and then eluted with SDS sample buffer before analysis by western blotting. Equal amounts of proteins were fractionated on SDS–polyacrylamide gels and blotted onto Hybond-ECL (GE Healthcare). After blocking with 4% Block Ace (Dainippon Seiyaku, Osaka, Japan), membranes were probed with relevant antibodies and developed with an ECL Plus Western Blotting Detection System (GE Healthcare) using a Fuji Film Image Scanner (LAS3000; Fuji Film, Tokyo, Japan).

Pulse-chase labeling assay

Cells were plated on a 10-cm dish and cultured until 70% confluence, after which the culture medium was changed to DMEM (met/cys-free) for 40 min at 37°C. After methionine depletion, 10% dialysed FBS (Invitrogen) containing 100 nmol/L PMA was added to the culture for 1.5 h. Cells were then radiolabelled for 2 h with pulse medium containing 1850 MBq/ml [^{35}S]-methiunine. The medium was removed and the labeling was terminated by the addition of normal culture medium. Radiolabelled protein was harvested by washing the cells three times with phosphate-buffered saline (PBS) and then lysing the cells in lysis buffer, as described above. Cell lysates were cleaned by centrifugation at 13 000 *g* for 10 min at 4°C. For immunoprecipitation, cell lysates were precleaned using 20 μL protein G sepharose (GE Healthcare) for 2 h. Then, 200 μg cleaned lysates was incubated with 0.5 μg anti-hILP/XIAP and 20 μL protein G sepharose with continuous rotation overnight at 4°C. Immunocomplexes were pelleted by centrifugation at 3500 *g* for 3 min at 4°C, washed in lysis buffer four times, and resuspended in 30 μL SDS sample buffer. Samples were boiled for 5 min and 15-μL aliquots were subjected to electrophoresis. Signals were detected and quantified using a densitometer (Fluor Chem IS-8000; Astec, Fukuoka, Japan).

Cell viability assay

The live/dead cell viability assay kit (Molecular Probes, Invitrogen, Carsbad, CA, USA) was used according to the manufacturer's instructions. Briefly, SH-SY5Y cells were grown on a 96-well plate (Iwaki, Tokyo, Japan) and treated with 0 or 100 nmol/L PMA for 1 h, following treatment with 0, 5 or 10 μg/mL etoposide for 24 h. After treatment of 25 μg/mL of etoposide for 24 h, SH-SY5Y cells, stably expressing wild-type XIAP or S87A XIAP, were pretreated with 0 or 1 μmol/L Gö6983 (Sigma) for 30 min and then treated with 0 or 100 nmol/L PMA for 1.5 h. After combined treatment, cells were then incubated with 2 μmol/L calcein AM and 4 μmol/L ethidium homodimer for 30 min at room temperature. Green fluorescent cells, resulting from mitochondrial cleavage of calcein AM, were counted as living cells and red fluorescent cells, resulting from binding of the cell-impermeable fluorescent dye ethidium homodimer to nuclei, were counted as dead cells using an All-one Type Fluorescence Microscope BZ8000 (KEYENCE, Osaka, Japan). The total cell population was calculated as the sum of living cells (green cytoplasm) with dead cells (red nuclei).

RESULTS

PKC phosphorylates XIAP at Ser^{87} *in vitro* and in cultured cells

As mentioned previously, XIAP has been shown to be phoshprylated by PKB,[12] and protein sequence analysis has evidenced that PKB and PKC share a common consensus phosphorylation sequence (RXXS/T) at residue Ser^{87} of XIAP. Thus, to examine whether PKC directly phosphorylates XIAP at Ser^{87} *in vitro*, we incubated recombinant XIAP and active PKC in a reaction mixture. The antibody against p-Ser^{87} XIAP specifically recognizes phosphorylated Ser^{87} in XIAP and, as shown in Fig. 1a, Ser^{87} was directly phosphorylated by PKC *in vitro*. We also used active PKB as a positive control to confirm phosphorylation at Ser^{87}.

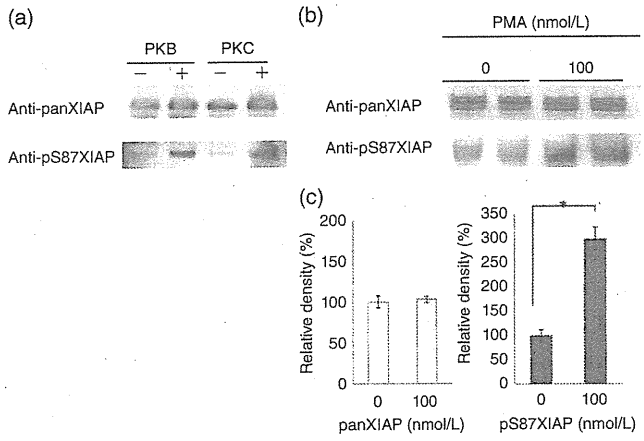

Figure 1 X-Linked inhibitor of apoptosis protein (XIAP) is phosphorylated by protein kinase C (PKC) at Ser^{87} *in vitro* and phorbol myristate acetate (PMA) increases phosphorylation of XIAP at Ser^{87} in cultured cells. (a) Recombinant XIAP was incubated with active PKC or PKB in the reaction mixture for 2 h at 37°C. Total XIAP was detected with anti-hILP/XIAP and phosphorylated Ser^{87} in XIAP was detected with anti-pSer^{87} XIAP. (b) Wild-type XIAP stably expressing SH-SY5Y cells were treated with and without PMA, as indicated, for 6 h followed by solubilization in lysis buffer. Lysateswere immunoprecipitated with anti-hILP XIAP mouse monoclonal antibody and immunoprecipitates were examined by western blot with rabbit polyclonal anti-C terminus XIAP antibody or rabbit polyclonal anti-pSer87 XIAP antibody. Representative data are shown. (c) The intensities of the bands immmunotained in the experiments of panel (b) (n = 6) were quantified, and mean and standard deviation (SD) were calculated. Therefore the data of anti-pan XIAP and anti-pS87 XIAP are corresponding to toal XIAP levels and phosphorylated XIAP in, respectively, in wild-type XIAP stably expressing SY5Y cells treated with and without PMA. *P < 0.02.

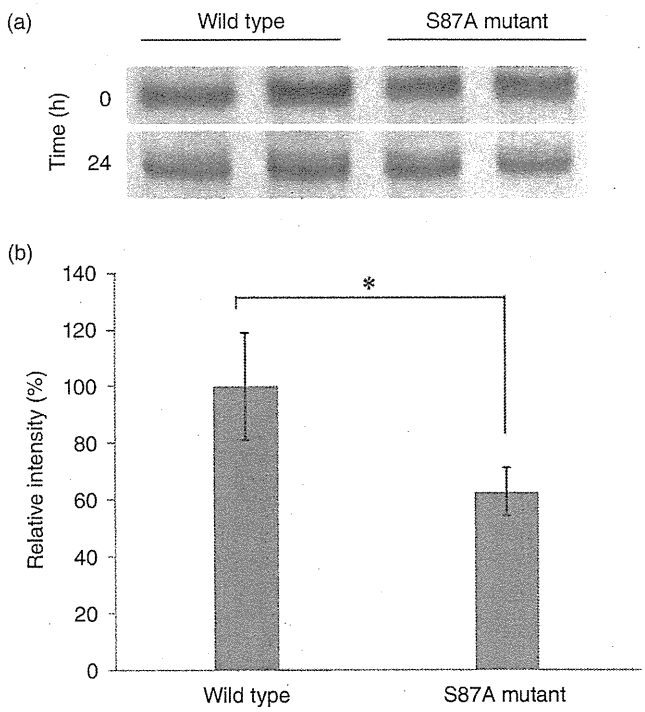

Figure 2 Phosphorylation of X-linked inhibitor of apoptosis protein (XIAP) at Ser^{87} increases its stability. Wild-type or S87A mutant XIAP stably expressing SY5Y cells treated with phorbol myristate acetate were radiolabeled for 2 h. Radiolabeled XIAP was immunoprecipitated with anti-hILP XIAP antibody, then subjected to sodium dodecyl sulfate–polyacrylamide gel electrophoresis. Signals were detected and quantified. Data are the mean ± SD. *P < 0.01.

Next, we examined the possibility of phosphorylation of XIAP at Ser^{87} by PKC in cultured cells. To activate PKC, we treated wild-type XIAP-expressing SH-SY5Y cells with 100 nmol/L PMA, a well known activator of PKC,[18,19] for 6 h. Total XIAP levels were constant among the samples, but p-Ser^{87} XIAP levels were increased in XIAP-expressing SH-SY5Y cells treated with PMA (Fig. 1b). Quantification of the data showed that PKC activation significantly increased phosphorylation of XIAP at Ser^{87} (Fig. 1c). These data indicate that XIAP is a physiological substrate for PKC.

PKC-phosphorylated XIAP at Ser^{87} has greater stability in SH-SY5Y cells

To determine whether specific phosphorylation of XIAP at Ser^{87} accounts for the stabilizing effect of PKC on XIAP levels, we performed pulse chase experiments. We transfected SH-SY5Y cells with wild-type XIAP and non-phosphorylatable S87A mutant XIAP, which was generated by converting the Ser^{87} residue to alanine. Cells were treated with PMA to activate PKC and then labeled metabolically with [^{35}S]-methionine. Immunoprecipitation was performed with anti-hILP/XIAP antibody and the same amount of labeled XIAP was visualized by SDS–polyacrylamide gel electrophoresis and autoradiography. As shown in Fig. 2a,b, non-phosphorylatable S87A mutant XIAP was degraded more rapidly than wild-type XIAP. The data suggest that PKC increases XIAP stability by phosphorylation of Ser^{87} in SH-SY5Y cells.

Phosphorylation of XIAP at Ser^{87} increases cell survival in etoposide-induced apoptosis

To examine whether increased XIAP stability after PKC activation protects cells from apoptosis, we exposed cells to etoposide, a topoisomerase inhibitor that causes mitochondrial damage followed by downstream caspase activation.[20] SH-SY5Y cells were pretreated with PMA to activate PKC and then incubated

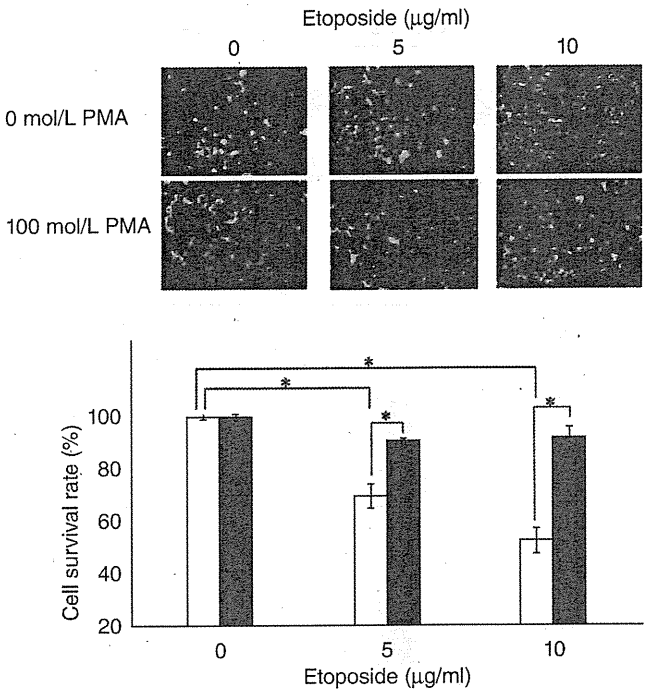

Figure 3 Phorbol myristate acetate (PMA) treatment increases the viability of SH-SY5Y cells after etoposide treatment. SH-SY5Y cells were exposed to 0, 5, or 10 μg/mL etoposide for 24 h after pretreatment with 0 or 100 nmol/L PMA. To distinguish living from dead cells, cells were incubated with 2 μmol/L calcein AM and 4 μM ethidium homodimer for 30 min at room temperature. Living cells (green) and dead cells (red) were visualized. In the lower graph, data are corrected for duplicate determinations from four independent experiments in the absence (□) and presence (■) of 100 nmol/L PMA and show the mean ± SD. *$P < 0.003$.

with etoposide to induce apoptosis. Cell survival was evaluated by the live/dead cell viability assay. Green fluorescent cells, resulting from mitochondrial cleavage of calcein AM, were counted as living cells and red fluorescent cells, resulting from binding of the cell-impermeable fluorescent dye ethidium homodimer to nuclei, were counted as dead cells. As shown in Fig. 3, PMA pretreatment prevented etoposide-induced cell death. Although SH-SY5Y cells that were not pretreated with PMA exhibited a dose-dependent reduction in cell survival rate after etoposide treatment, PMA-treated SH-SY5Y cells had a significantly higher cell survival rate. This suggests that PMA-dependent activation of PKC protects cells against etoposide-induced apoptosis.

Next, we evaluated whether this cell protection after PMA treatment depended on specific phosphorylation of XIAP at Ser^{87} by PKC. Thus, wild-type or S87A mutant XIAP-expressing cells were exposed to etoposide (Fig. 4) in the presence and absence of PMA and the cell survival rate was determined. We verified that, in both groups, the cell survival rate was reduced to 30% after exposure to etoposide. However, treatment with PMA significantly rescued wild-type XIAP-expressing SH-SY5Y cells from apoptosis, but not cells expressing the S87A XIAP mutant.

Furthermore, pretreatment of PMA-treated cells with the PKC specific inhibitor Gö6983 completely suppressed the PMA-associated rescue of cell survival in wild-type XIAP-expressing SY5Y cells exposed to etoposide (Fig. 4.).

These results suggest that specific activation of PKC protects cells, at least in part, against apoptosis induced by etoposide by specific phosphorylation of XIAP at Ser^{87} (Fig. 5).

DISCUSSION

There is growing evidence that PKC plays essential roles in the brain. The PKC family is composed of classical (cPKCs; PKCα, PKCβ, and PKCγ), novel (nPKCs; PKCδ, PKCε, PKCη, and PKCθ) and atypical (aPKCs; PKCζ and PKCλ) PKC isoforms. Among these PKCs, PMA activates cPKCs and nPKCs. Of relevance to AD, PKC can activate α-secretase.[21–23] The activation of α-secretase results in the cleavage of amyloid precursor protein ether directly by activation of PKC isozymes α and ε, or by indirect activation of extracellular signal-regulated kinase 1/2.[21–23] Phorbol ester-induced activation of α-secretase apparently involves translocation of PKCα from the cytosol to the membrane compartment and translocation of PKCε from the cytosol to Golgi-like structures.[24] Conversely, β-amyloid peptide (Aβ) can inactivate PKC: Aβ contains a putative PKC pseudosubstrate site (Aβ28-30) that is critical for a direct interaction between Aβ and PKC.[25] It has been reported that $Aβ_{1–40}$ degrades PKCα in nomal human fibroblasts and PKCγ in AD patient fibroblasts.[26] Addition of $Aβ_{1–40}$ peptide to cultured B103 cells reduced the activated forms of PKCα and PKCε. It is also inhibited phorbol ester-induced membrane translocation of PKCα and ε without altering their expression levels, indicating that activation of intracellular PKC is inhibited by treatment with Aβ peptide.[24] In addition, PKC has been shown to inhibit the formation of AD-related neurofibrillary tangles, which are composed of highly phosphorylated tau, via inactivation

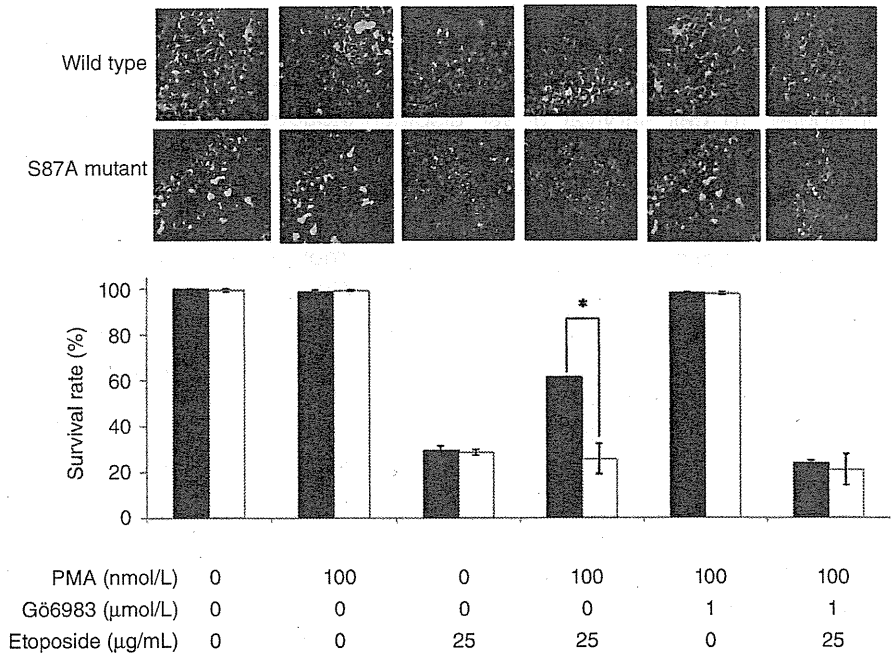

Figure 4 Phosphorylation of X-linked inhibitor of apoptosis protein (XIAP) at Ser^{87} by protein kinase (PK) C protects cells against apoptosis induced by etoposide. Wild-type or Ser87A mutant XIAP stably expressing SH-SY5Y cells were pretreated with 1 mmol/L Gö6983 for 30 min and then treated with 0 or 100 nmol/L phorbol myristate acetate (PMA) for 1.5 h, followed by the induction of apoptosis with 25 μg/mL etoposide. To distinguish living from dead cells, cells were incubated with 2 μmol/L calcein AM and 4 μmol/L ethidium homodimer for 30 min at room temperature. Living cells (green) and dead cells (red) were visualized. Data are corrected for triplicate determinations from two independent experiments and show the mean ± SD in the wild-type (■) and S87A mutant (□) groups. *$P < 0.002$.

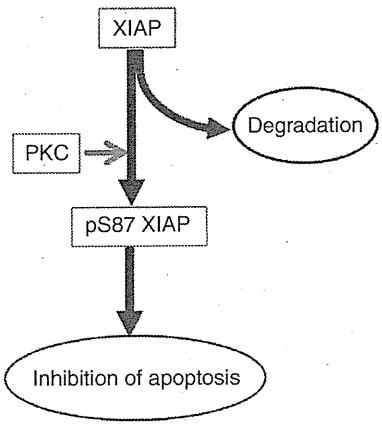

Figure 5 Phosphorylation of X-linked inhibitor of apoptosis protein (XIAP) at Ser^{87} by protein kinase (PK) C increases cell viability. In living cells, XIAP is degraded, whereas XIAP phosphorylated at Ser^{87} escapes the degradation processes and suppresses apoptotic cell death.

of glycogen synthase kinase 3 (GSK3), a well-known tau kinase.[27] An immunohistochemical study revealed PKCλ/ι within tau-positive neurofibrillary inclusions in AD, progressive supranuclear palsy, corticobasal degeneration, and Pick disease, within α-synuclein-positive Lewy bodies in idiopathic Parkinson's disease and dementia with Lewy bodies, as well as within glial inclusions in multisystem atrophy.[28] In addition, PKCλ/ι is closely associated with the inactivated form of GSK3β.[29] Although many studies have been undertaken to assess the role of PKC in amyloid precursor protein (APP) processing and tau phosphorylation, evidence of a direct relevance of PKC in cell survival has not been provided.

In the present study, we investigated whether PKC activation modulates XIAP stability through phosphorylation of Ser^{87} and, thus, affects cell survival. Our data demonstrate that PMA-dependent activation of PKC leads to XIAP phosphorylation at Ser^{87} (Fig. 1), which stabilizes XIAP levels (Fig. 2), leading to increased SH-SY5Y cell survival after etoposide treatment (Fig. 3). Substitution of the serine residue with alanine at position 87 (S87A) markedly attenuated protection of cell survival after PMA induction (Fig. 4), indicating that the Ser^{87} epitope is a specific target of PKC, playing a role in cell survival under stressful conditions. To further validate the specific contribution of PKC activation in the protection against etoposide-induced apoptosis, we pretreated wild-type XIAP-expressing SH-SY5Y cells with the PKC specific inhibitor Gö6983 prior to treatment with PMA and etoposide. The failure to rescue cell survival with PMA after pretreatment with Gö6983 supports the notion that specific PKC activation is required for XIAP-directed cellular protection against apoptosis.

It has been shown in small lung cancer cells that overexpression of PKCε increases XIAP levels and cell viability through the formation of a specific multipro-

tein complex that comprises B-Raf, PKCε, and S6K2 and promotes cell survival.[30] In addition, phosphorylation of XIAP at Ser[87] by PKB stabilizes XIAP and contributes to cell survival under cisplatin-induced apoptotic conditions in A2780S ovarian cancer cells.[12] Thus, it is possible that PKC function is impaired in AD pathology, affecting neuronal survival through abnormal control of XIAP stability. Although numerous studies have shown a neuroprotective role of PKC by activation of α-secretase,[31–33] a direct effect of PKC-dependent XIAP phosphorylation on cell survival had not been reported to date.

Our results are consistent with previous work in which the anti-Parkinson/monoamine oxidase (MAO)-B inhibitor rasagiline decreased apoptosis by upregulation of PKCα and PKCε mRNA[34]. Downregulation of XIAP induced by serum starvation appears to be mediated by inactivation of the PKCα/β pathway.[35] We have demonstrated previously that treatment of SH-SY5Y cells with $A\beta_{1-42}$ lowered levels of XIAP. The addition of $A\beta_{1-40}$ peptide to cultured B103 cells reduced the activated forms of PKCα and PKCε.[24] We have not identified the specific isoform(s) of PKC that may be responsible for the results in our experiments and this remains to be elucidated.

Although AD pathology involves not only amyloid burden, but also other aging or inflammatory factors leading to stress conditions, our finding of involvement of PKC in the regulation of XIAP may be helpful for understanding the vulnerability in neuronal cells in the AD brain. In fact, significantly decreased PKC activity has been reported in the aged rat brain,[36] therefore increased vulnerability of neuronal cells in the aged brain may be explained, in part, by decreased PKC activity through its phosphorylation of XIAP.

In summary, our results support the importance of PKC, through phosphorylation of XIAP at Ser[87] and its stabilization, in cellular survival under stressful conditions that may lead to apoptosis in neuronal cells. Further studies are needed to elucidate the role of this neuroprotective in differentiated neurons exposed to stressful conditions, such as $A\beta_{1-42}$, and in the brain of AD patients, as well as to identify the specific PKC isoform involved in this process.

ACKNOWLEDGEMENTS

The authors would like to thank Dr Antonio Currais (CNB-S, The Salk Institute, CA, USA) for help with the English expression and helpful comments on this article. This work was supported, in part, by Grants from the Ministry of Education, Culture, Sports, Science, and Technology of Japan (No. 21390333 and no. 20591407).

REFERENCES

1 Kermer P, Liman J, Weishaupt JH, Bahr M. Neuronal apoptosis in neurodegenerative diseases: From basic research to clinical application. *Neurodegener Dis* 2004; **1**: 9–19.
2 Rothe M, Pan MG, Henzel WJ, Ayres TM, Goeddel DV. The TNFR2–TRAF signaling complex contains two novel proteins related to baculoviral inhibitor of apoptosis proteins. *Cell* 1995; **83**: 1243–1252.
3 Duckett CS, Nava VE, Gedrich RW *et al.* A conserved family of cellular genes related to the baculovirus iap gene and encoding apoptosis inhibitors. *EMBO J* 1996; **15**: 2685–2694.
4 Liston P, Roy N, Tamai K *et al.* Suppression of apoptosis in mammalian cells by NAIP and a related family of IAP genes. *Nature* 1996; **379**: 349–353.
5 Ambrosini G, Adida C, Altieri DC. A novel anti-apoptosis gene, survivin, expressed in cancer and lymphoma. *Nat Med* 1997; **3**: 917–921.
6 Hauser HP, Bardroff M, Pyrowolakis G, Jentsch S. A giant ubiquitin-conjugating enzyme related to IAP apoptosis inhibitors. *J Cell Biol* 1998; **141**: 1415–1422.
7 Bartke T, Pohl C, Pyrowolakis G, Jentsch S. Dual role of BRUCE as an antiapoptotic IAP and a chimeric E2/E3 ubiquitin ligase. *Mol Cell* 2004; **14**: 801–811.
8 Deveraux QL, Takahashi R, Salvesen GS, Reed JC. X-linked IAP is a direct inhibitor of cell-death proteases. *Nature* 1997; **388**: 300–304.
9 Roy N, Deveraux QL, Takahashi R, Salvesen GS, Reed JC. The c-IAP-1 and c-IAP-2 proteins are direct inhibitors of specific caspases. *EMBO J* 1997; **16**: 6914–6925.
10 Takahashi R, Deveraux Q, Tamm I *et al.* A single BIR domain of XIAP sufficient for inhibiting caspases. *J Biol Chem* 1998; **273**: 7787–7790.
11 Yamamori H, Tanaka T, Kudo T, Takeda M. Amyloid-beta down-regulates XIAP expression in human SH-SY5Y neuroblastoma cells. *Neuroreport* 2004; **15**: 851–854.
12 Dan HC, Sun M, Kaneko S *et al.* Akt phosphorylation and stabilization of X-linked inhibitor of apoptosis protein (XIAP). *J Biol Chem* 2004; **279**: 5405–5412.
13 Van Huynh T, Cole G, Katzman R, Huang KP, Saitoh T. Reduced protein kinase C immunoreactivity and altered protein phosphorylation in Alzheimer's disease fibroblasts. *Arch Neurol* 1989; **46**: 1195–1199.
14 Wang HY, Pisano MR, Friedman E. Attenuated protein kinase C activity and translocation in Alzheimer's disease brain. *Neurobiol Aging* 1994; **15**: 293–298.
15 Masliah E, Cole G, Shimohama S *et al.* Differential involvement of protein kinase C isozymes in Alzheimer's disease. *J Neurosci* 1990; **10**: 2113–2124.
16 Kimura T, Yamamoto H, Takamatsu J, Yuzuriha T, Miyamoto E, Miyakawa T. Phosphorylation of MARCKS in Alzheimer disease brains. *Neuroreport* 2000; **11**: 869–873.
17 Shi RX, Ong CN, Shen HM. Protein kinase C inhibition and X-linked inhibitor of apoptosis protein degradation contribute to the sensitization effect of luteolin on tumor necrosis factor-related apoptosis-inducing ligand-induced apoptosis in cancer cells. *Cancer Res* 2005; **65**: 7815–7823.